DISCOVERER

PERFORMANCE ANALYSIS REPORT
FLIGHT OF FTV-1029 (u)

(30-DAY REPORT)

13 AUGUST 1959

CONTRACT AF 04 (647)-97

LMSD-445053 2 SEPTEMBER 1959

[redacted]

UNCLASSIFIED

LMSD-445053
2 September 1959
Copy No. C-41
38 Sheets

DISCOVERER PROGRAM
PERFORMANCE ANALYSIS REPORT
FLIGHT OF FTV-1029 (u)

13 AUGUST 1959

(30-DAY REPORT)

CONTRACT AF 04(647)-97

Approved:

R Smelt
R. Smelt, Manager
Satellite Systems

J R Hollenbeak for
E. R. Proctor, Manager
Program Administration and Control
Satellite Systems

LOCKHEED AIRCRAFT CORPORATION
Missiles and Space Division
Sunnyvale, California

UNCLASSIFIED

REPORT CHANGE RECORD

FOR

The following changes and/or additions should be incorporated into the document identified above. This Report Change Record page itself should be inserted as the first page of the affected report (preceding the title page). If any pages in the original document are to be eliminated and/or replaced by the instructions which follow, those pages should be destroyed according to the Air Force Directive governing such destruction.

REPORT CHANGE NUMBER: LMSD-445053 (Errata Page 3) Replaces Errata Page 1
CONTRACT NUMBER: AF 04(647)-97

ERRATA (CORRECT IN INK)			
LMSD NO.	PAGE NO.	CORRECTION	CORRECTION MADE (INITIAL AND DATE)
445053	✓ xi	SUMMARY: last sentence, para. 4, change flight-path angle from .02 degree to .01 degree.	
	✓ 5-1	SECTION 5: Fig. 5-1, change insertion angle from .02 degree to .01 degree	
	✓ 5-2	SECTION 5: Fig. 5-2, change flight-path angle for Agena engine burnout from .02 degree to .01 degree.	
		OK 9/21/59 mle	

LOCKHEED AIRCRAFT CORPORATION
Missiles and Space Division
Sunnyvale, California

REPORT CHANGE RECORD

FOR

The following changes and/or additions should be incorporated into the document identified above. This Report Change Record page itself should be inserted as the first page of the affected report (preceding the title page). If any pages in the original document are to be eliminated and/or replaced by the instructions which follow, those pages should be destroyed according to the Air Force Directive governing such destruction.

REPORT CHANGE NUMBER: LMSD-445053
CONTRACT NUMBER: AF 04-(647)-97

ERRATA (CORRECT IN INK)			
LMSD NO.	PAGE NO.	CORRECTION	CORRECTION MADE (INITIAL AND DATE)
445053	✓5-1	Fig. 5-1, change Insertion Altitude from 134 to 137	
	✓7-6	Fig. 7-3, add note under Propulsion Pre-flight nominal as follows: (1) Based on oxidizer runoff	
✓	7-6	Fig. 7-3, change (1) for 1018 under W_f column, Propulsion Post-flight Data, to I_{sp} column	
✓	7-6	Fig. 7-3, change for 1022 and 1023 under Thrust Term. column from Typ. Com. and Non Deter., respectively, to Prop. Exh.	
✓	9-3	After the word "b" in line 8 under Horizon Scanner, insert the following: ± 8.2 degrees maximum at apogee, gradually decreasing to essentially zero at points	

LOCKHEED AIRCRAFT CORPORATION
Missiles and Space Division
Sunnyvale, California

UNCLASSIFIED

FOREWORD

This performance analysis report has been prepared by the Lockheed Aircraft Corporation, Missiles and Space Division, in compliance with Contract AF 04(647)-97, dated 19 December 1957.

The purpose of the report is to present major problem areas of Discoverer Agena flight test performance and conclusions reached. Included in the report are evaluation of flight records and the results of analytic postflight investigations. In the interest of making the information available as soon as possible after the flight, the report publication time (commencing with this report) was reduced to 20 days, instead of 30 days as provided in the contract.

Compilation and overall system performance analysis integration were made by personnel of Department 62-42, Data Control and Analysis. Analyses and evaluation from the Project Design Departments of the Satellite Systems Project are an integral part of this report.

SECRET UNCLASSIFIED

LMSD-445053

DISCOVERER AGENA RE-ENTRY

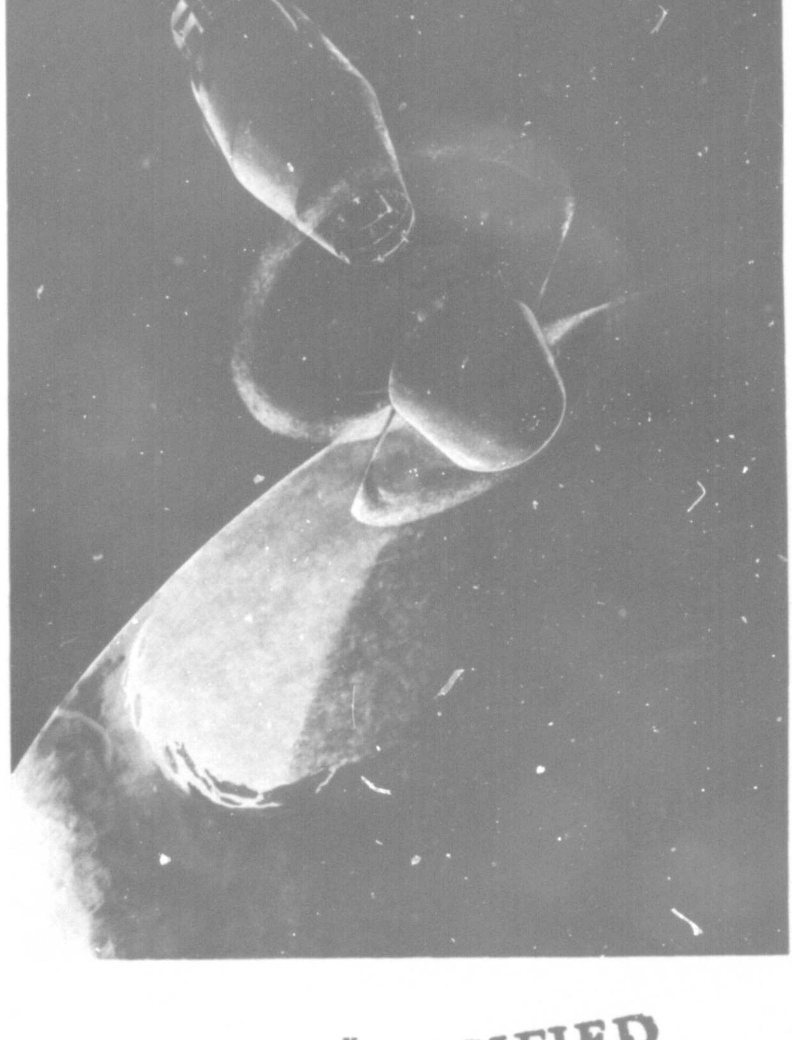

UNCLASSIFIED

LOCKHEED AIRCRAFT CORPORATION SECRET MISSILES and SPACE DIVISION

CONTENTS

ILLUSTRATIONS

ILLUSTRATIONS (Continued)

SUMMARY

Discoverer V, consisting of Agena Flight Test Vehicle 1029, Model 2205, and Thor Booster SM-75 Serial No. 192 was successfully launched on 13 August 1959 from Complex SM-75-3, Pad 4, at Vandenberg Air Force Base, California.

After liftoff, the first-stage booster lofted the Agena vehicle approximately 17 miles higher-than-nominal and 1 degree east of the predicted track in azimuth. First mode bending oscillations experienced on previous launches were absent.

The Vandenberg AFB VERLORT radar experienced periodic dropouts while tracking; however, the Point Mugu radar tracking was excellent and the velocity-to-be-gained and time-to-fire commands were properly received and executed.

Orbital boost was normal, and although engine performance was again marginal, orbit status was achieved. Engine shutdown was not commanded by the integrator but occurred due to propellant exhaustion. Had command shutdown been achieved by the integrator, an excessive orbit period would have resulted. Orbital injection occurred at a velocity of 25,973 ft/second and a flight-path angle of 0.01 degrees with perigee altitude of 137 statute miles and apogee of 456 statute miles. An orbital period of 94.2 minutes was computed with a lifetime for the satellite of approximately 48 days.

Orbital performance and acquisition of the Agena vehicle were achieved on all in-range passes by the remote tracking stations. Reset commands were transmitted and executed during Orbits 1 and 2; attempts to reset

the orbital timer period on Orbit 9 by Annette was unsuccessful; however, reset was accomplished on Orbits 10 and 16 passes. Capsule ejection occurred and was verified by Hawaii tracking on the Orbit 17 pass, but recovery was not accomplished due to incomplete electro-mechanical sequencing within the capsule.

Subsequent orbital radar sightings of the Agena vehicle were obtained. Nineteen days of orbital life and 292 orbits have been completed as of 1 September 1959. Orbital decay is occurring at a rate calculated to attain the predicted orbital life of 48 days.

DISCOVERER FLIGHTS SUMMARY

Discoverer Designation	Flight No. Designation	Agena FTV Serial No.	Thor Booster Serial No.	Launch Date	Vehicle Changes Incorporated	Remarks
-	1	1019	160	1-21-59	-	Malfunction during countdown caused ullage rockets, retro-rockets, separation bolts, and horizon scanner fairing to fire when hydraulic motor was turned on. Design problem. Launch was aborted.
I	2	1022	163	2-28-59	Hydraulic motor circuit separated from pyrotechnics circuit.	Injection angle -2.5° caused lifetime of under seven days. No telemetry or radar orbit contacts made. Sporadic doppler sightings. Vehicle believed damaged structurally and/or thermally at injection or during first pass.
II	3	1018	170	4-13-59	UDMH fuel incorporated. Horizon scanner active during engine burning phase, and gains altered to tighten control system.	Engine shutdown by command - source unknown - believed due to relay malfunction. Orbit achieved. Capsule ejected but not recovered. Two weeks lifetime
III	4	1020	174	6-3-59	Fairchild Timer incorporated. More severe environmental testing of engine relay box. Selected unit installed in vehicle.	Premature engine burnout due to fuel exhaustion. Insufficient velocity for orbit attainment. Question of proper loading of propellants and possible fuel line leaks. Under nominal performance by Agena engine but within specifications.
IV	5	1023	179	6-25-59	None	Premature engine burnout believed due to vortexing of fuel. Insufficient velocity for orbit attainment. Under nominal performance by Agena engine but within specifications.
V	6	1029	192	8-13-59	Vehicle weight reduced. Fuel slosh screens removed. Vortex suppressor installed. RJ-1 fuel used in Thor. Delta V increased to yield elliptical orbit and longer period.	Successful launch and orbit although lower than nominal performance of engine. Injection angle +0.02°, perigee 137 statute miles, apogee 456 statute miles, 48 days estimated life. Capsule separations on orbit 17. No recovery.

BLANK PAGE

CONCLUSIONS

STRUCTURES AND ENVIRONMENT (SUBSYSTEM A)

First mode bending oscillations experienced on previous flights were eliminated by relocation of the Thor gyro package to a more rigid structure in the booster forward equipment area. Launch criteria will be revised to reflect the elimination of these oscillations.

PROPULSION (SUBSYSTEM B)

The subnormal performance of the orbital engine is undergoing further investigations to determine more specific causes for the lower-than-nominal performance. Additional instrumentation is being studied as a requirement to fully define this problem area.

AUXILIARY POWER SUPPLY (SUBSYSTEM C)

The Primary Power source continued to deliver operative level voltages to the telemeter transmitter through Orbit 26, approximately 1030 watt-hours excess over predicted battery life. A revaluation of the power requirements is being conducted to determine if the power capability can be safely reduced.

GUIDANCE AND CONTROL (SUBSYSTEM D)

Additive errors in the Reeves Computer and the vehicle integrator resulted in a final total error of 168 ft/second. Investigations are being conducted into the possibility of applying nominal or proportional compensation of command lines to correct this condition.

GROUND-SPACE COMMUNICATIONS (SUBSYSTEM H)

The periodical dropout of the Vandenberg AFB VERLORT radar was due to both an unbalanced elevation signal error amplifier and interference, which caused the antenna to increase in elevation whenever the beacon return was outside of the receiver gate. Investigation reveals that several powerful radars were illuminating the vehicle beacon and were disabling it more than the VAFB VERLORT could tolerate. It will be necessary to obtain frequency protection during the first 500 seconds after launch in order to eliminate interference.

INSTRUMENTATION

Loss of commutated Channel 12 temperatures after Orbit 2 was attributed to failure of the differential amplifier. This is considered a random failure; therefore, no remedial action is planned.

RECOVERY RESEARCH CAPSULE (SUBSYSTEM L)

The failure of the capsule electronic circuits to properly sequence after initial separation and retro-fire is believed due to low temperature effect on the mercury batteries which prevented normal power generation. The outer coating of paint on the ablative shell will be removed before the next flight. It is believed that this will permit a temperature rise, sufficient for normal battery functioning.

SECTION 1
INTRODUCTION AND OBJECTIVES

INTRODUCTION

The Lockheed Aircraft Corporation, Missiles and Space Division, is assigned Prime Contractor responsibility for the Discoverer Space System (Satellite Systems Project). This program, which is under the authority of the Department of Defense, is directed by the Advanced Research Projects Agency and administered by the Air Force Ballistic Missile Division of the Advanced Research Development Command, the contracting agency. The purpose of the Discoverer Space Program is to use a large satellite vehicle (Agena) as a scientific-data-gathering medium.

This report is primarily concerned with analyses of major problem areas of Agena Flight Test Vehicle (FTV) 1029 which was the fifth satellite-booster configuration launched under the Discoverer Program. The FTV-1029 was configured to include an instrumented recoverable capsule and the physical means to effect capsule re-entry and recovery. The Agena underwent captive firing tests at the Santa Cruz Test Base on 16 May 1959 and was subsequently delivered to Vandenberg Air Force Base for final assembly and checkout, mating with the Thor booster, and launching. The launch was successfully accomplished on the sixth countdown attempt on 13 August 1959.

TEST OBJECTIVES

Objective	Accomplished			Remarks
	Yes	No	Part	
Primary				
Demonstrate orbit capability of the Agena/Thor and evaluate the component systems:	X			
a. Ground Support Equipment	X			
b. Thor Booster	X			
c. Agena Satellite:				
1. Airframe and Adapter	X			
2. Propulsion System			X	Subnormal performance in I_{sp} and total impulse
3. Auxiliary Power Unit System	X			
4. Guidance and Control Systems	X			
5. Telemetry, Tracking, and Command System	X			VAFB tracking was erratic during ascent
6. Ejection and Reentry	X			Separation of capsule occurred as programmed
7. Recovery System (Task Force)			X	Task force deployed and functioned but recovery not accomplished
Secondary				
Interrelations of satellite structure and systems	X			
Environmental data			X	Channel 12 - internal web and skin temperatures lost after second orbit
Interstation communications	X			
Station acquisition	X			
Aerodynamic integrity of Agena/Thor combination	X			Bending oscillations eliminated
Telemetry monitoring of secondary data	X			
Tertiary				
Crew and ground equipment evaluation from the human engineering point of view	X			

SECTION 2
CONFIGURATION

The Agena/Thor Discoverer V configuration (Fig. 2-1) consisted of a second-stage orbital satellite (Agena), Model 2205, Serial No. 1029 in tandem with a modified IOC Thor booster SM-75, DM-13, Serial No. 192. The combined length of Discoverer V was approximately 80 feet; the total fueled weight at liftoff was 117,153 pounds.

CONFIGURATION MODIFICATIONS

Thor Booster

The Douglas Thor booster configuration was identical to the Discoverer IV Serial No. 172 configuration, with the following exceptions:

a. The booster was powered by a modified MB-2, Block I, Rocketdyne propulsion system.

b. The Block I system incorporated systems modifications that permitted faster engine-start sequence with a shorter liftoff time and smaller cutoff impulse.

Agena

The Agena vehicle, Model 2205, Serial No. 1029 was basically the same as FTV-1023 (Discoverer IV), with the following exceptions (see Fig. 2-2):

a. Approximately 51 pounds were removed from the vehicle as listed in Ref. 3

b. The propulsion system (SS/B) consisted of YLR-81-BA-5 rocket engine Serial No. 105

c. The screen balls previously used in FTV-1023 were removed and replaced with a system of three screen balls for the purpose of reducing vortex formation in the fuel and oxidizer tanks.

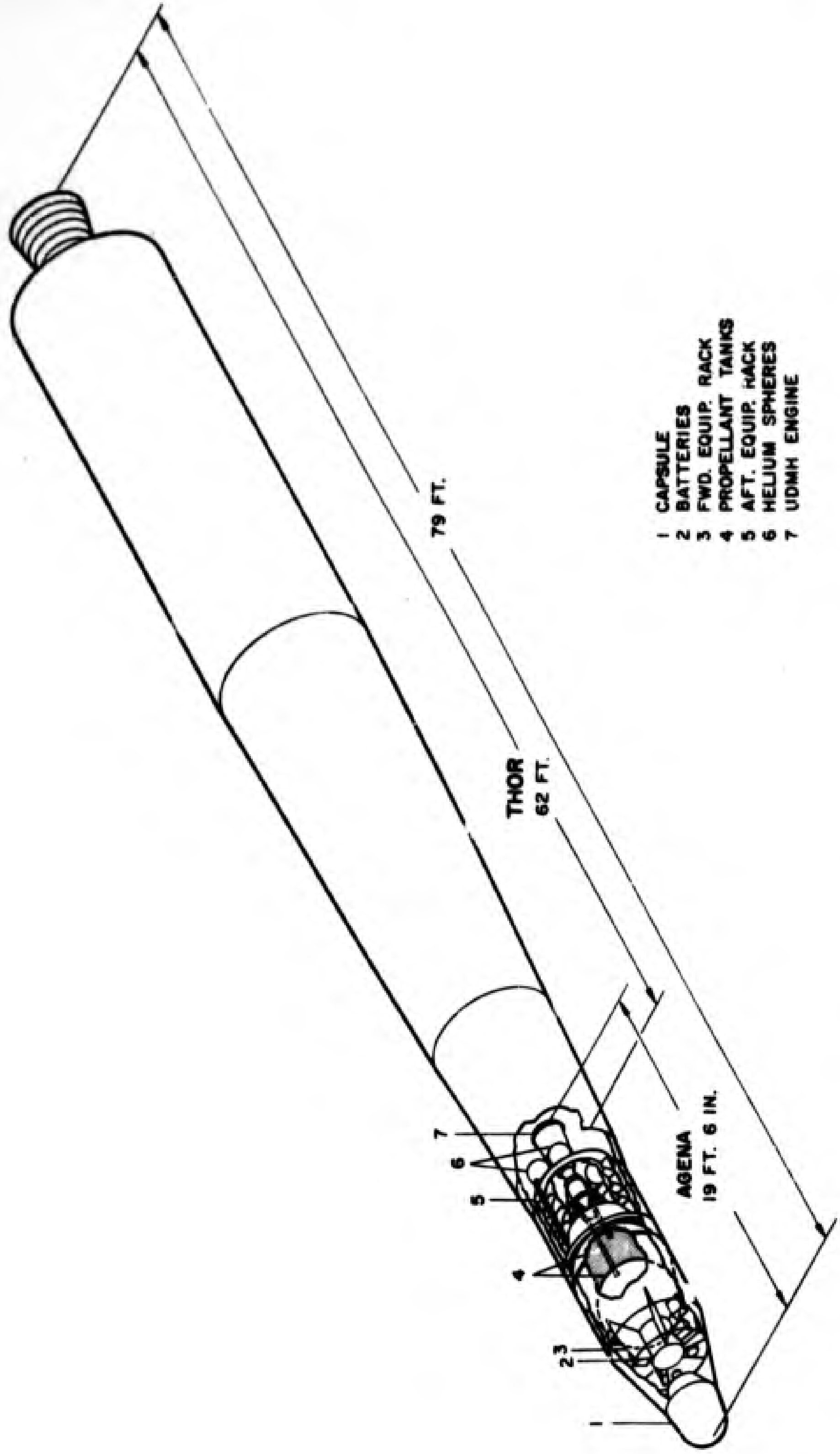

Fig. 2-1 Discoverer Agena/Thor Perspective View

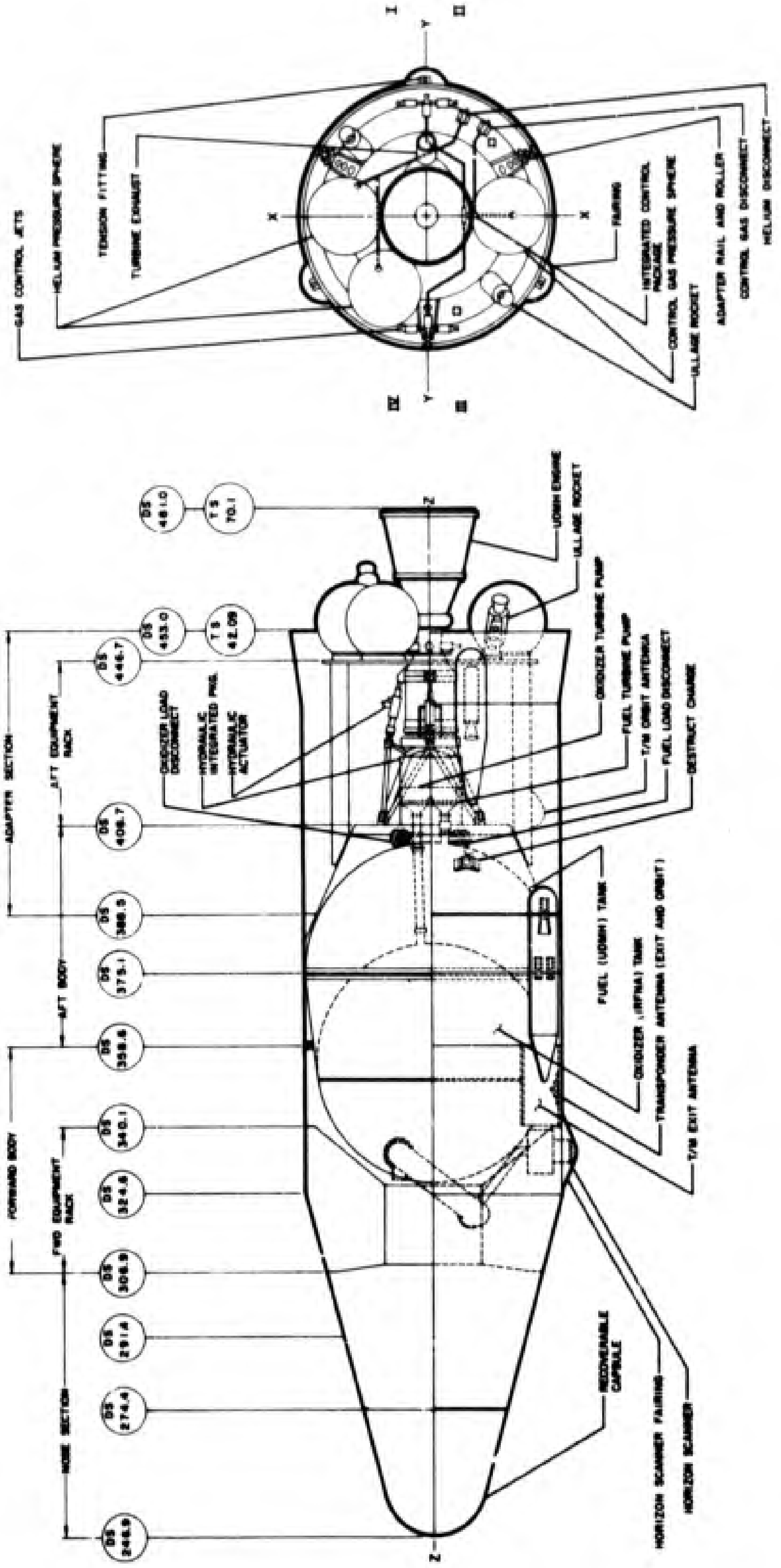

Fig. 2-2 Discoverer Agena Inboard Profile, FTV-1029

BLANK PAGE

SECTION 3

LAUNCH SEQUENCE OF EVENTS

Discoverer Satellite FTV-1029

Lift-off Time 1200:07.41 PDT Flight Date: 13 August 1959

Event	Flight Time Actual (sec)	Flight Time Predicted (sec)	Remarks (From T/M data)
Lift-off 107831.41 (System Time, sec)	0	-	Thor lift-off tone and A_z, Channel 9
Thor Main Engine Cutoff	161.70	164.0	Thor MEP_c and longitudinal accelerometer
Gyros Uncaged	-	167.0	Pitch, roll and yaw gyros, Channels 15-11, 15-15, and 15-19
Thor Vernier Engine Cutoff	170.8	173.0	Thor vernier chamber pressure
N_2 Valve Opened	178.59	178.0	N_2 regulated pressure, Channel 14-2
Explosive Bolts Fired	178.59	178.0	Explosive bolts monitor, Channel 17-15
Pneumatic Control Activated	179.59	178.0	SS/D timer monitor, Channels 15-3 and 14
Retro Rockets Fired	179.79	179.0	Approx. times - T/M Dropout
Separation Began	179.79	179.0	Approx. times - T/M Dropout
Start Fairchild Timer	179.79	179.0	Approx. times - T/M Dropout
Separation Completed	180.5	-	Separation monitor, Channel 6
45°/min Nose-down Pitch Rate	192.5	192.0	Pitch gyro torque, Channel 15-12
Power Off to N_2 Valve and Separation Monitor	192.55	192.0	Separation monitor, Channel 6

Event	Flight Time Actual (sec)	Flight Time Predicted (sec)	Remarks (From T/M Data)
Horizon Scanner Shroud Squibs Fired	192.5	192.0	No monitor
Horizon Scanner Signal Connected to Pitch and Roll Gyros	220.0	221.0	Pitch and roll gyros, - pitch torque signal interferes - no data
2^{o}/min Nose-down Pitch	221.5	221.0	Pitch gyro torque, Channel 15-12
Beacon Command No. 5 Given (SS/D Timer Brake On, Timer Stopped)	221.96	-	Beacon verification, Channels 16-7 and 16-9
Beacon Command No. 6 Given (Velocity Correction)	256.33	-	Beacon verification, Channels 16-7 and 16-9, duration 5.17 seconds
Ullage Rockets Fired	270.29	269.37	No monitor
Hydraulic Pump Motor	270.29	269.37	Hydraulic pressure, Channels 14-17 and SS/D timer monitor, Channels 15-3 and 14
Beacon Command No. 6 OFF	261.50		Beacon verification, Channels 16-7 and 16-9
Gas Generator Squibs Fired (Engine Ignition)	286.32	285.37	Gas generator squib monitor, Channels 17-3 and 18
Helium Bypass Squib Fired	286.32	285.37	Gas generator squib monitor, Channel 17-16
Power Off to Gas Generator Squib and H_e Bypass Valve Circuits	287.3	-	Gas generator squib monitor, Channel 17-3; and squib monitor, Channel 17-16
Thrust Attained	287.70	-	Combustion chamber pressure, Channel 13 and A_z, Channel 9
Engine Shutdown	403.19	-	Combustion chamber pressure shutdown relay, Channel 13 and A_z, Channel 9

Event	Flight Time Actual (sec)	Flight Time Predicted (sec)	Remarks (From T/M Data)
Oxidizer, Fuel, and Helium Vent Valve Squibs Fired	414.49	413.37	Squib monitor, Channel 17-16
Hydraulic Motor Shutdown	414.49	413.37	SS/D Timer monitor, Channel 15-3
40°/min Nose-Right Yaw Rate	414.49	413.37	Yaw gyro torque, Channel 15-25
0°/min Pitch Rate	414.49	413.37	Pitch gyro torque
Switched to T/M Phase 7 (Switch Antennas	-	-	Continuous T/M channels OFF
T/M Signal Lost (Mugu)	484.0	-	
T/M Signal Lost (VAFB)	474.6	-	
4°/min Nose-up Pitch Rate	684.29	683.37	Pitch gyro torque
Horizon Scanner Roll Signal Connected to Yaw Gyro	684.29	-	T/M signal lost
Integrator Shutdown	684.39	-	Velocity monitor
T/M Signal Lost (Pvt. Joe E. Mann)	775.0	-	
Telemetering Off	-	-	No information

SECTION 4
GROUND SUPPORT EQUIPMENT

Attempts were made to launch Agena FTV-1029 on 28, 29, and 30 July and on 11, 12, and 13 August. The history and operational details of the six launch attempts were reported in Appendix II of Ref. 3. A review of subsequent data and information revealed that the following events occurred:

During the launch attempt of 11 August, a Helium leak occurred. This leak was found to be in the Asco solenoid valve on the acid vent system. The leakage was not great enough to prevent a successful launch, but after the flight was cancelled because of weather, a new valve was installed.

The lanyard on the air conditioning duct was broken after a successful disconnect during the 13 August launch.

The following modifications (made since the flight of Agena FTV-1023) functioned as designed:

a. The sequence disconnect of the temperature control blanket operated satisfactorily, first releasing from the vehicle and then from the mast.

b. The air conditioning duct dampers prevented the blast from entering the umbilical trench.

c. The single-stage umbilical disconnect performed as designed and release was accomplished in 0. 59 second after the lift-off signal.

SECTION 5
DISCOVERER FLIGHT PERFORMANCE

This section covers the post-flight performance estimates and trajectory simulation of Agena vehicle FTV-1029, from Thor burnout to orbital boost burnout. Performance of the Thor is covered in a separate report supplied by Douglas Aircraft Corp.

Simulations, using the Point Mugu Mod-II radar-trajectory data, were obtained for both the coast phase and orbital boost and agree closely with radar data. See Fig. 5-1.

Injection Conditions	Orbit Parameters
Insertion Altitude (statute miles)	[redacted] 137
Insertion Latitude (degrees)	24° 6.8' N
Insertion Angle (degrees)	0.[redacted] 01 (9/18/59-mli)
Insertion Velocity (feet-per-second)	25,973
Period (minutes)	94.2
Perigee Altitude (statute miles)	137
Apogee Altitude (statute miles)	456
Orbit Inclination (degrees)	80
Eccentricity	0.04
Vehicle Lifetime (days)	48
Mean Altitude (statute miles)	296

Fig. 5-1 Summary of Orbital Elements

Coast Flight Simulation

The coast-flight simulation was obtained by making a best fit to the Point Mugu radar position data. Figure 5-2 gives pertinent trajectory data at various points on the coast trajectory and Figs. 5-3 and 5-4 show the results of the coast-flight simulation.

Event	Flight Time (sec)	Radar Altitude (ft)	Range (ft)	Flight Path Angle (deg)	Inertial Velocity (ft/sec)
Thor Main Engine Burnout	161.7	269,600	477,000	19.5	13,710
FTV-1029 Agena Engine Ignition	287.7 (90% P_c)	655,600	1,988,000	7.7	12,796
Thor Coast Apogee	360.0	714,000	2,840,000	0	12,654
FTV-1029 Agena Engine Burnout	403.2	726,972	3,968,000	0.01	25,973

Fig. 5-2 FTV-1029 Burnout Conditions

The simulation indicates the Thor booster trajectory was lofted approximately 17 statute miles. Part of the lofting was because of the higher-than-predicted flight-path angle at Thor main engine cutoff.

Orbital Boost Simulation

Upon completion of the coast-phase simulation, the actual time of FTV-1029 engine ignition and the actual average propellant flow rate were used to obtain the orbital-boost simulation. A specific impulse of 272.6 seconds yielded the best simulation of radar position data.

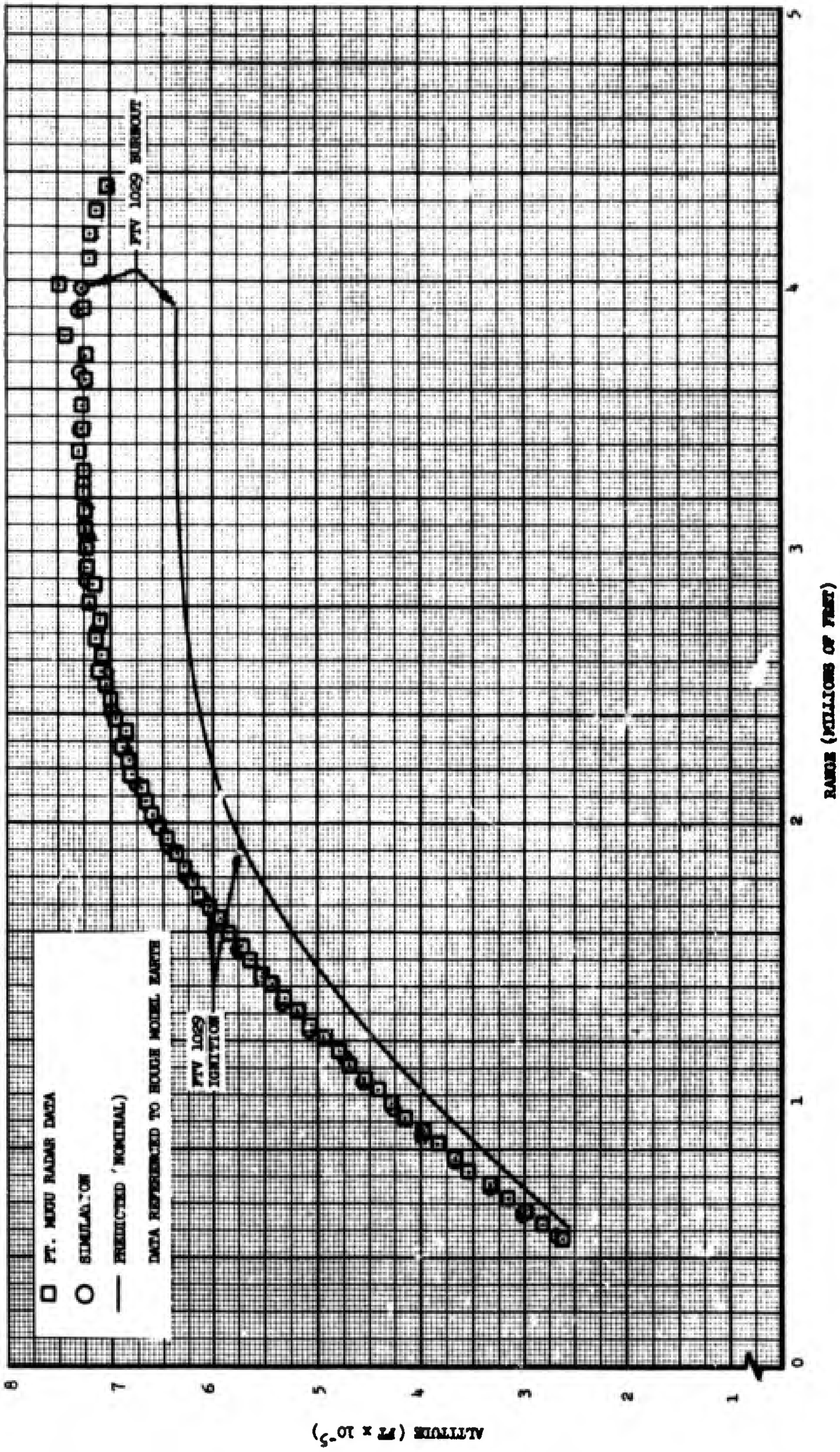

Fig. 5-3 Agena Launch Trajectory, Altitude vs Range

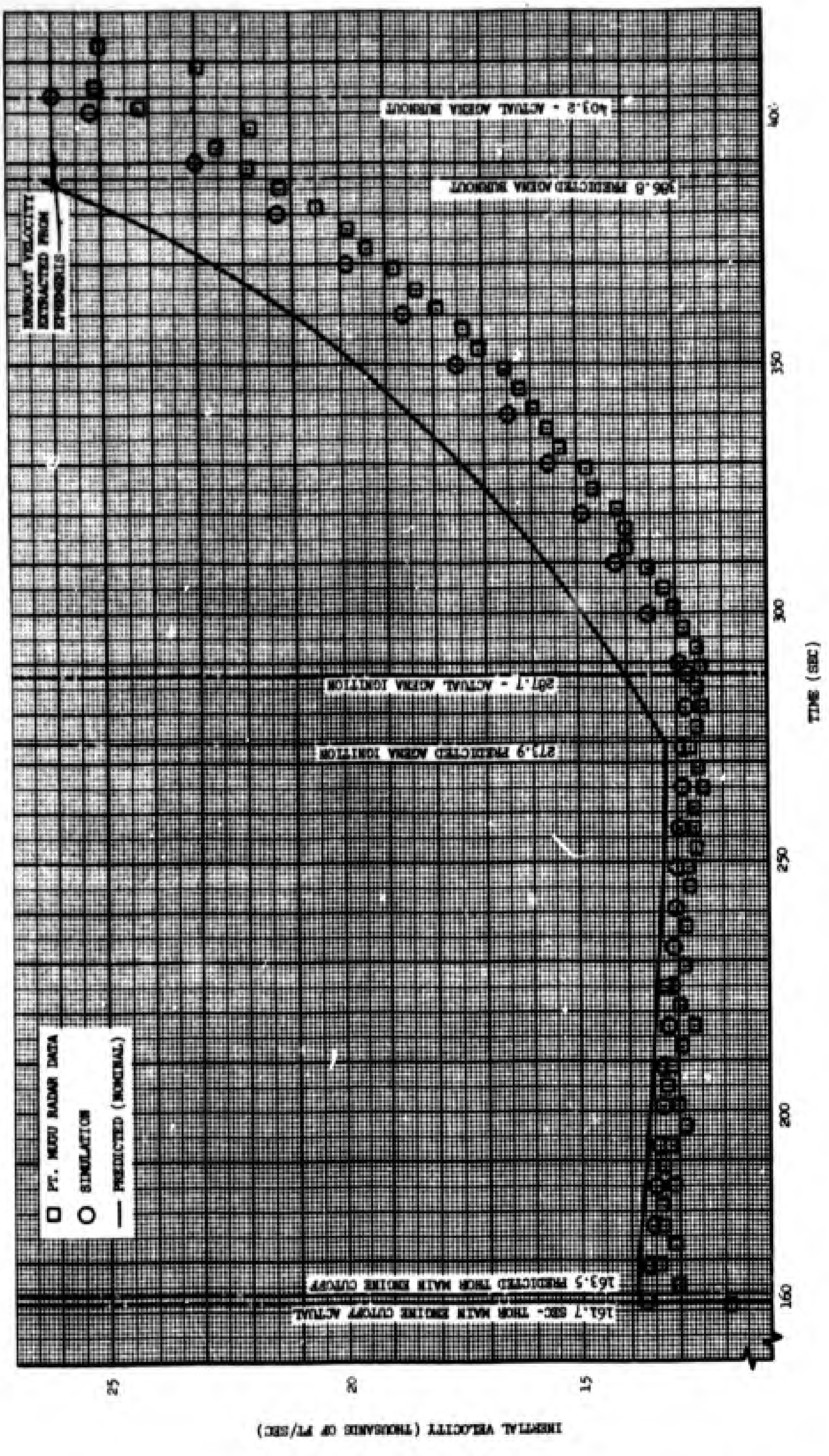

Fig. 5-4 Agena Launch Trajectory, Velocity vs Time

SECTION 6
STRUCTURES AND ENVIRONMENT (SUBSYSTEM A)

AIRFRAME AND ADAPTER

Launch

Contributions of flexible bending moments to total flight loads during atmospheric boost were negligible. First bending mode yaw oscillations which occurred in previous Agena flights were not present. The elimination of these oscillations is due to relocation of the Thor rate gyro package to a more rigid structure in the booster forward equipment area.

The consistent occurrence of yaw oscillations during the previous flights resulted in reduction of launch criteria based on available Thor engine angle. Revision has been made to this criteria reflecting the elimination of these oscillations.

Propellant Slosh

Indication of propellant slosh was not apparent during orbital boost from records of engine actuator position, missile accelerations, gyros or rate gyros. The screen balls previously used as propellant damping devices in the UDMH tank were removed in FTV-1029. These damping devices were replaced by a system of three screen balls for the purpose of reducing vortex formation. The net baffle weight savings was 13 pounds. This significant vehicle design change appears to be proven out by evaluation of the data of FTV-1029.

SHOCK AND VIBRATION ENVIRONMENT

The instrumentation tabulated below was installed on FTV-1029 (Fig. 6-1). This instrumentation is similar to that installed on FTV-1023 and comments made in Ref. 1 are also applicable here.

Channel	Location (sta)	Sensitive Axis Orientation	Transducer	Transducer Range (g)	Frequency Response (cps)	Data Frequency Response (cps)
7	409	Yaw Plane	Statham-A501T Ca	±3	0-100	0-45
8	409	Pitch Plane	Statham-A501T Ca	±3	0-100	0-50
9	409	Longitudinal	Statham-A501T Ca	±15	0-300	0-80
18	320	Longitudinal	Glennite-A321 AHT	±35	10-2000	20-1750

Fig. 6-1 Shock and Vibration Instrumentation

Vibration Environment

Because of its high-frequency capability, the forward vibration transducer (Channel 18) is used primarily to define the vibration environment in the 500-1500 cps frequency range. Although this channel is capable of recording vibration occurring below 500 cps, experience has shown that the vibration magnitude in the lower frequency range is below the background noise level of this channel. As mentioned in Ref. 8, a close similarity exists between the high-frequency vibration environment which occurs during the first few seconds of flight and that which occurs during the vehicle static firings. This has been further verified through more recent test firings. Figure 6-2 shows the similarity between flight data from FTV-1029 and FTV-1023 and the static firing of FTV-1023.

A much more extensive survey of the high-frequency vibration was made during static firings than was possible during actual flight. The results of this survey, coupled with this noticed similarity, have been used to more precisely define the vibration test levels to be used for this program.

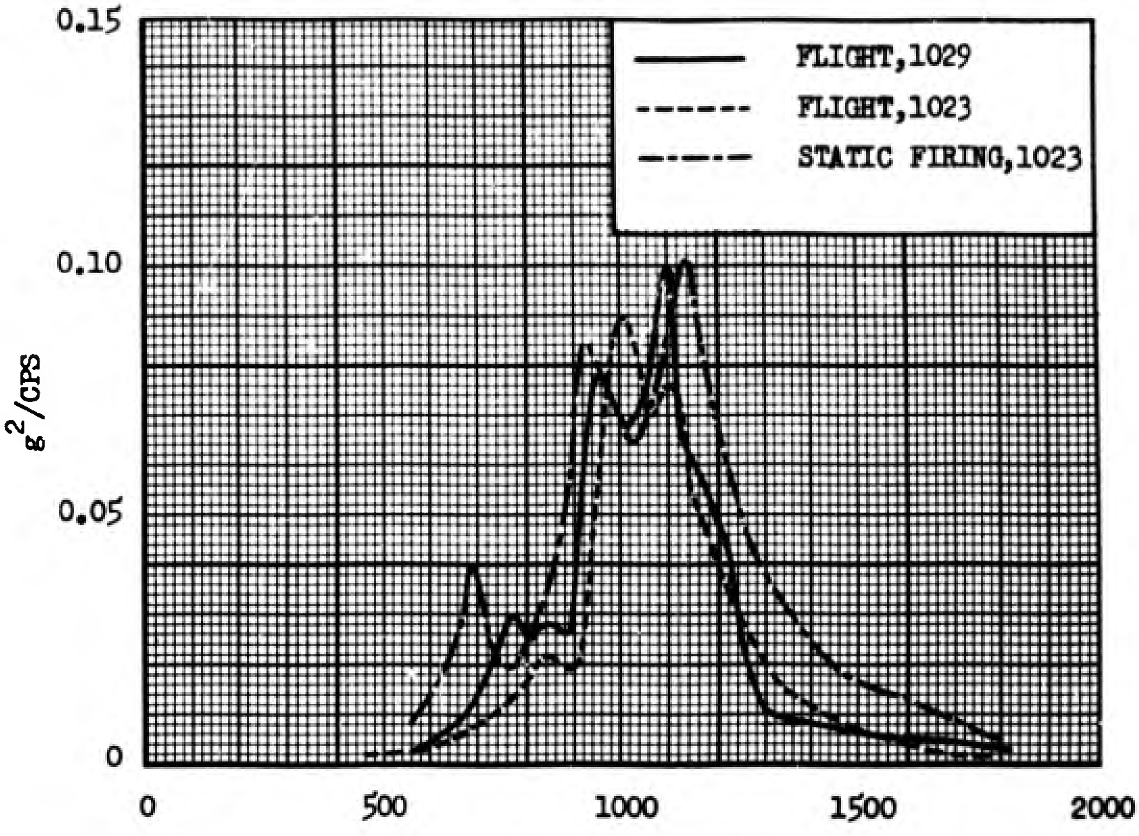

Fig. 6-2 High Frequency Vibration Comparison FTV-1029 and FTV-1023

These test levels now appear in Ref. 4. As more extensive flight vibration instrumentation becomes available (scheduled for the MIDAS Agena series), more accurate test levels can be determined and will be incorporated into the applicable specifications.

During FTV-1029, as on all previous flights, significant high-frequency vibration was recorded at liftoff and again during the transonic region, with liftoff typically the more severe of the two periods. The level of high-frequency vibration during second-stage ignition is too low to determine quantitative magnitude. However, this level is considerably lower than the level recorded during liftoff.

Aft Accelerometers

The most significant period of low-frequency vibration occurred for a period just after second-stage ignition (287 to 330 seconds). The vibration was approximately 1 g in the pitch and yaw planes but was not of a significant magnitude along the logitudinal axis. Lateral vibration of this duration has not been recorded on previous flights.

A longitudinal shock, varying from 1.5 g forward to 3 g aft, occurred at second-stage shutdown. The most severe pitch and yaw response during these two shocks was only slightly greater than 1 g. These shock conditions are considerably less severe than those used for design or test.

WEIGHT AND BALANCE

The propellant loading weight, center-of-gravity, and moment-of-inertia data are presented in Figs. 6-3 and 6-4.

Propellant	Subtotal (lb)	Total (lb)
Oxidizer Loaded		4,766
Impulse	4,696	
Preflow	21	
Unusable	49	
Fuel Loaded		1,865
Impulse	1,822	
Allowance for Mixture Ratio	14	
Unusable	29	
Total Propellant Load		6,631

Fig. 6-3 Propellant Loading

Condition	Weight (lb)	CG Z	Location X	Inches Y	Moments-of-Inertia, Slug - ft^2		
					I_{xx}	I_{yy}	I_{zz}
Liftoff	117,153	798.6	+0.03	+0.07	803,194	803,191	3,293
Booster Burnout	17,720	655.0	+0.21	+0.30	394,395	394,393	2,175
Thor Payload	8,593	362.2	-0.03	+0.06	2,157	2,172	155
Separation	8,434	361.1	-0.03	+0.06	2,003	2,021	130
Engine Ignition	8,389	360.0	-0.01	+0.06	1,916	1,933	126
Burnout	1,846	353.5	0	+0.28	1,523	1,551	126
End of Orbit	1,726	349.9	+0.18	+0.32	1,424	1,439	124

Fig. 6-4 Weights, Center-of-Gravity, and Moments-of-Inertia Summary

TEMPERATURE ENVIRONMENT

Flight data were obtained from seven of the eleven installed skin-temperature sensors during ascent and from four of the eleven during the first two orbit passes (one of the eleven was severed prior to first-stage separation). In general, all measured data were well below predicted values. Conduction to adjacent internal heat sinks is believed to have significant effect which necessitates having temperature sensors far removed from internal heat sinks to properly evaluate the aerodynamic heat transfer prediction method.

Analysis of the flight temperature data indicated that the equipment in the forward equipment rack was operating well within specified limits during ascent and throughout the orbital phase. Channel 12, which includes most of the temperature instrumentation components, failed sometime between Orbit 2 and Orbit 9. Consequently, temperature data from this channel were not obtained beyond Orbit 2. Orbit temperature data were obtained for the beacon transponder through Orbit 16 and for the battery case through Orbit 17.

Skin Temperature

Skin temperature data for the ascent phase were obtained from launch to approximately 780 seconds of the flight of FTV-1029. Skin temperature data were also obtained for 500 seconds in Orbit 1 and for 200 seconds in Orbit 2. A tabulation of the locations of the eleven skin temperature sensors is presented in Fig. 6-5. Of these eleven skin temperatures, three thermocouples (SD39, SD40, and SD41) failed to produce any valid data. No data were reduced for SD47. Also, orbit data were not reduced for SD74 and SD82. SD65 is disconnected at separation from the first-stage, therefore, could not produce data in orbit.

Measurement Number	Type*	Instrument Range (°F)	Vehicle Station	Skin Thickness (inches)
SD39	T	0 to 2000	275.22	0.100
SD40	T	0 to 2000	279.65	0.100
SD41	T	0 to 2000	291.95	0.100
SD45	R	-100 to 600	327.0	0.071
SD46	R	-100 to 600	350.0	0.071
SD47	R	-100 to 600	356.5	0.071
SD48	R	-100 to 600	379.5	0.112
SD65	R	-100 to 600	445.0	0.125
SD66	R	-100 to 600	338.0	0.071
SD74	R	-100 to 300	326.3	0.071
SD82	R	-100 to 300	326.3	0.071

* T represents thermocouple
R represents resistance thermometer

Fig. 6-5 Skin Temperature Sensor Location

Figure 6-6 presents the maximum skin temperatures recorded by the skin temperature sensors, as read from faired data curves. The figure shows that the maximum skin temperatures were below 300°F.

Equipment Rack Temperatures

Temperature sensors were located on the temperature sensitive components which are tabulated in Fig. 6-7. In addition, a number of resistance thermometers were located on the structural webs, the internal skin surface, and the inner cylinder. Temperature data were obtained for all except two of the sensors during the launch phase of flight (the telemeter transmitter temperature indication failed at launch and beacon temperature data were not reduced).

Ascent Heating

During ascent, temperature data for the instrumented components were recorded to 750 seconds after launch.

The maximum equipment temperatures recorded during ascent were safe and well below specified maximum operating temperatures, as shown in Fig. 6-7. This figure also indicated that the temperatures were still within safe limits after an arbitrary zero shift increase in temperature was applied.

The ascent temperature rise obtained during flight is also shown in Fig. 6-7. For purpose of comparison, the temperature rise expected (due only to internal power dissipation) is also presented. In general, it appears that a significant portion of the equipment temperature rise is because of component power dissipation.

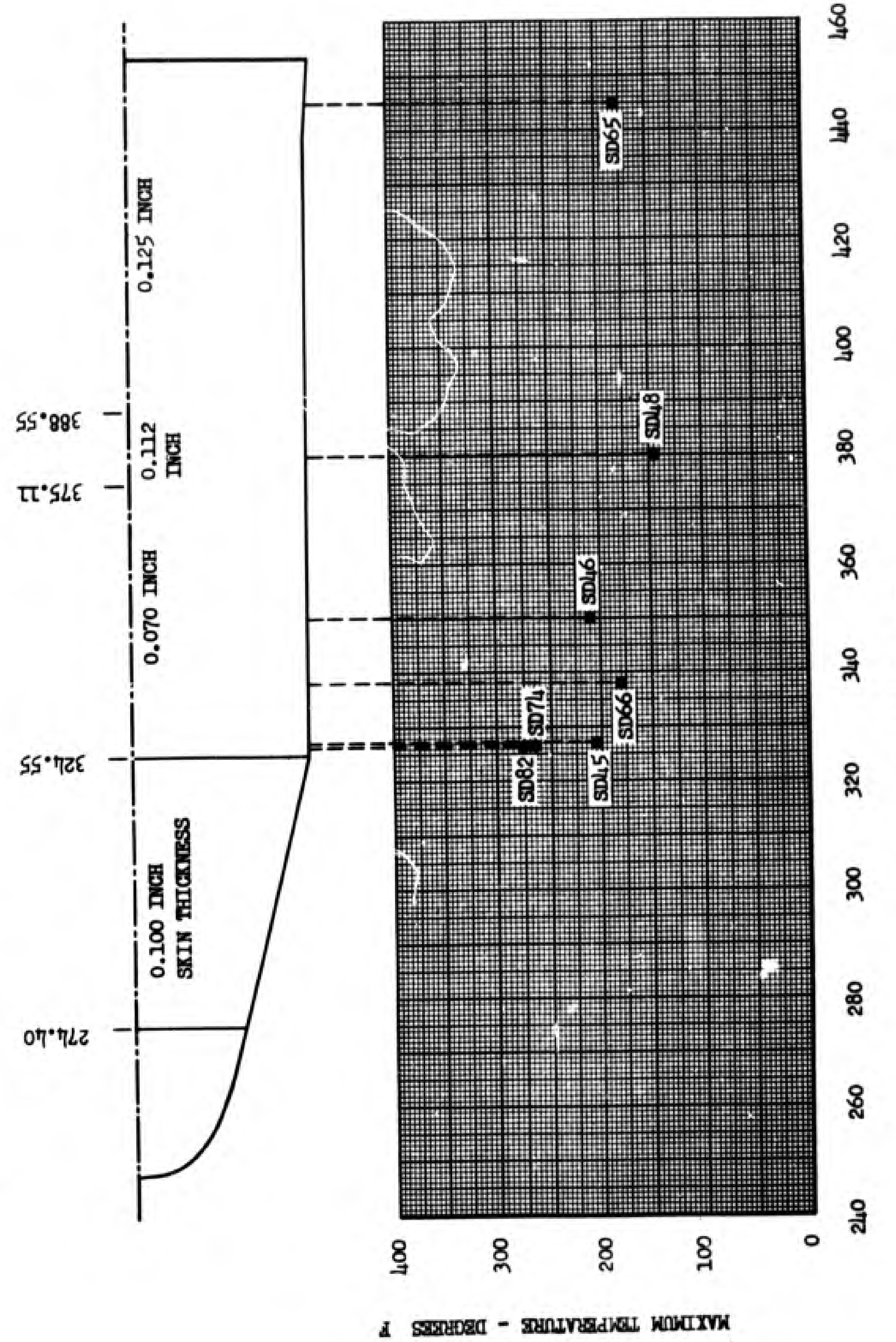

Fig. 6-6 Maximum Measured Skin Temperature

Instrumentation		Temperature At Launch		Temperature During Ascent		Temperature Rise During Ascent 0 - 750 Seconds		Temperature During Orbit Orbit Readout				
Component	Sensor	Telemeter Data (°F)	Predicted Value (°F)	Maximum Temperature (°F)	Maximum Allowable Temperature (°F)	Flight Data (°F)	Due to Power Dissipation Only (°F)	#1	#2	#9	#16	#17
2000 cps Inverter	SD80	37(2)	61	85 108*	140	48	19.5	66	62	---	---	---
Beacon Transponder	H74	---	62	70	145	--	18	78	67	57	67	---
Battery Case	C9	61	45-50	86	100	25	2(1)	---	76	75	---	89
Horizon Scanner	D82	35(2)	65	45 69*	140	10	4.5	62	67	---	---	---
Telemeter Case	SD81	37(2)	61	71 93**	---	34	--	54	47	---	---	---
Guidance Electronics	D60	59	90-105	70	125	11	5.8	---	70	---	---	---
Gyro Block	D61	140	162 ±5	140	**	--	--	122***	112	---	---	---
Inner Cylinder (TM Bay)	SD92	40(2)	50-75	96	---	--	--	---	45	23	---	43
Inner Cylinder (IRP Bay)	SD89	53	50-75	76	---	--	--	---	78	57	---	67
Skin (Cylindrical Section) (Inverter Bay)	SD82	44	50-75	276	---	--	--	---	-12	-22	---	---
Skin (Cylindrical Section) (IRP Bay)	SD74	68	50-75	263	---	--	--	---	34	0	---	28.5

*Temperatures Resulting from Zero Shift Correction
**Gyro Block Main Heater Set for 162 ±5°F
***Gyro Block Auxiliary Heater Set for 135°F

(1) Bulk average temperature rise (includes effect of weight of battery plus case).
(2) These values are not considered valid. They are lower than the cooling air temperature (44°F).

Fig. 6-7 Instrumentation Temperature Histories

Orbit Operation

The available orbit temperature data indicated that the instrumented electronic components were operating within specified operating temperatures (Fig. 6-7) throughout the orbital phase.

A thermal analyzer network program was used to predict vehicle skin temperature in orbit; a nominal 120-mile, circular, noon orbit was assumed. Two typical skin section temperature predictions from this program are shown in Fig. 6-8 along with the corresponding flight data for the Orbit 2 readout. The actual mean orbit altitude was about 200 miles higher than that used in the program. As a result, the vehicle encountered lower albedo and earth shine heat rates than had been calculated. Nevertheless, good correlation appeared between expected and measured temperatures. Note that the slopes are simlar. Also, observe that the vehicle skin farthest from the earth experienced the largest temperature excursion. Lack of temperature data prevents a more thorough analysis.

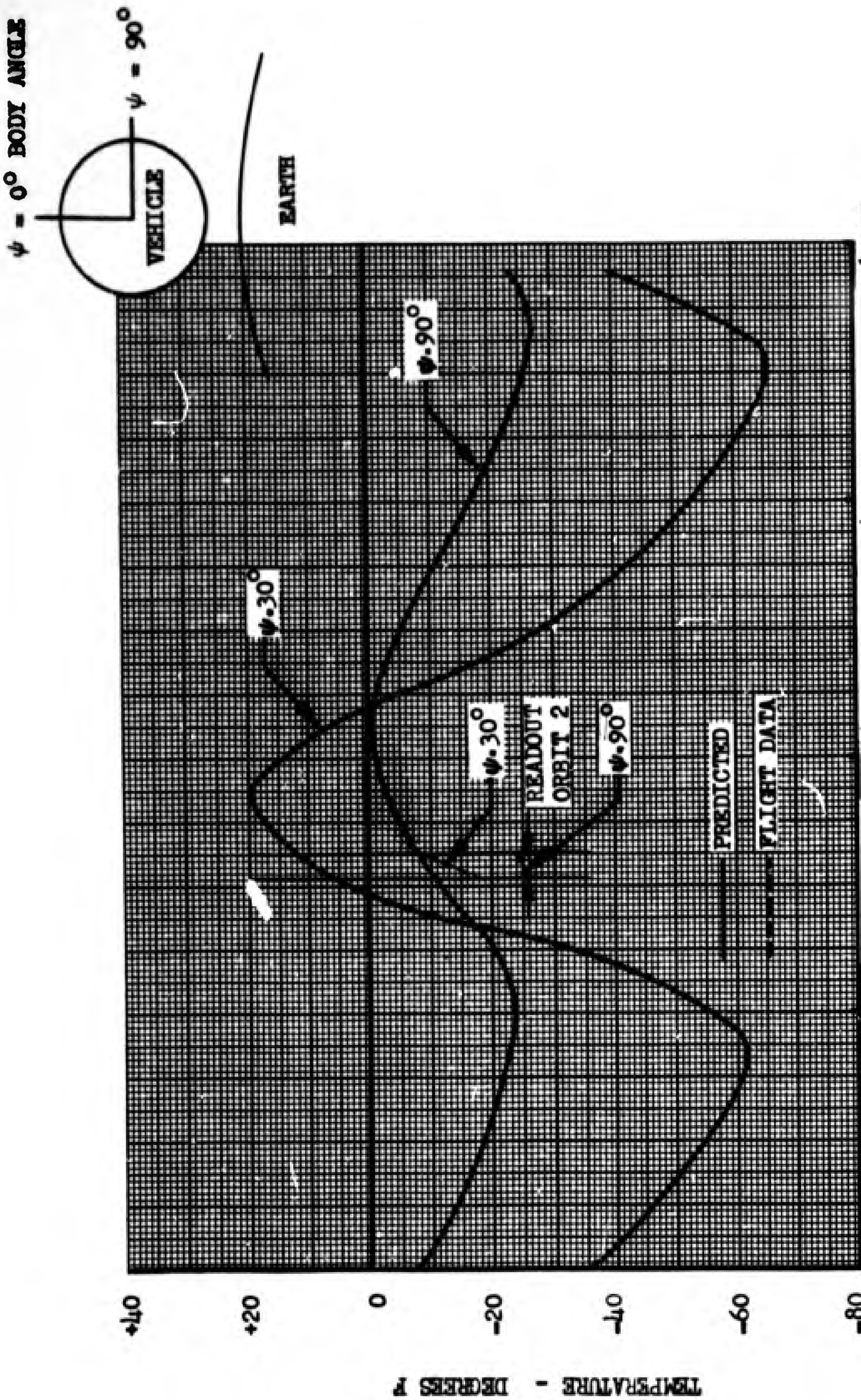

Fig. 6-8 Cylinder Skin Temperatures - Orbits 1 and 2 (Equipment Bay)

SECTION 7
PROPULSION (SUBSYSTEM B)

Engine Performance Analysis

Propulsion subsystem performance values are shown in Fig. 7-1. The performance analysis is based on velocity increments obtained from the acceleration integrator and from the trajectory simulation and propellant flow rates obtained from the telemetered data. Specific impulse and total impulse are determined from,

$$I_{sp} = \frac{\Delta V}{g \ln \frac{W_o}{W_{bo}}} \qquad (1)$$

and

$$I_t = I_{sp} (W_o - W_{bo}) \qquad (2)$$

where ΔV = velocity increment contributed by the engine during thrust duration time, ft/sec

W_o = Vehicle weight at ignition (90% thrust), lb

W_{bo} = Vehicle weight at burnout, lb

$$W_{bo} = W_o - \dot{W}_T (t) \qquad (3)$$

W_T = Average total propellant flow rate, lb/sec

t = Thrust duration time, seconds

I_{sp} = Specific impulse, lb-sec/lb

I_t = Total impulse, lb-sec.

Performance Characteristics	Specification	Pre-Flight Prediction	Actual
1. Velocity Increment, ft/sec	-	13630 Available	13320 (1)
2. Thrust Duration, sec	120 ±6	115.1	115.49
3. Total Oxidizer Loaded, lb	4761	-	4766
4. Total Fuel Loaded, lb	1864	-	1865
5. Total Propellants Loaded, lb	6625	-	6631
6. Oxidizer Specific Gravity at 60°F	1.568 (nom)	-	1.568
7. Fuel Specific Gravity at 60°F	0.795 (nom)	-	0.7945
8. Oxidizer Temperature, °F	60° (max)	-	52 to 59
9. Fuel Temperature, °F	60° (max)	-	54 to 62
10. Thrust Chamber Pressure, psia	500 (nom)	511	491 (1) 498 (2)
11. Engine Thrust, lb	15160-15910	15930	15408 (1) 15610 (2)
12. Specific Impulse, sec	280 (min)	282	273 (1) 276.5 (2)
13. Total Impulse, lb/sec	-	1.833×10^6	1.78×10^6 (1) 1.80×10^6 (2)
14. Oxidizer Flow, lb/sec	-	40.77	40.73
15. Fuel Flow, lb/sec	-	15.71	15.73
16. Total Propellant Flow, lb/sec	-	56.48	56.46
17. Turbine Speed, rpm	-	24950	24670
18. Helium Supply Pressure, psia	3000 at 120°F at liftoff	-	3000 decays to 500
19. Oxidizer Tank Pressure, psia	-	58	60
20. Fuel Tank Pressure, psia	-	58	59
21. Oxidizer Pump Inlet Pressure, psia	40 (min)	63-74	66-73
22. Fuel Pump Inlet Pressure, psia	34 (min)	57-58	57-59
23. Oxidizer Pump Lip Seal Pressure, psia	2-18	-	17 to 13
24. Thrust Attainment Time, sec	1.3 - 1.9	-	1.36
25. Thrust Overshoot, %	50% (max)	-	22
26. Thrust Chamber Pressure, Prior to Ignition, psia	-	5.5	5.5

(1) Calculated using a velocity increment by simulation of radar position data
(2) Based on telemetered thrust chamber pressure

Fig. 7-1 Propulsion Subsystem Performance, FTV 1029

Considering the velocity increment to be accurate (since the integrator and trajectory simulation are in very close agreement) and the initial vehicle weight to be accurate, then determination of system performance is subject to error in the propellant flow rate. An error analysis was performed to determine the error of the flow rate measurement as calculated by the turbine speed method. The analysis indicates that the computation will yield total flow rates to within an error of approximately 1.2 percent. Figure 7-2 shows the effect of flow rate errors on the indicated subsystem performance as determined from the preceding equations. The "performance line" describes the locus of points that satisfy equations 1, 2, and 3 when 13,290 ft/sec is used as the ΔV term and when 8,362 lb is used as the W_o term. To discount the effect of ullage rockets and cutoff impulse on engine steady state performance, 30 ft/sec was subtracted from the observed value of velocity increment.

Calculated flow rates indicate that 19 pounds of usable fuel were remaining at shutdown and that 9 pounds of the non-usable oxidizer were burned. These values are not too significant because they are subject to large errors, caused by the accumulation of the flow rate error.

Figure 7-2 shows that the observed performance was at a lower level than predicted. But, considering errors in the calculated burnout weight, determination of whether the low performance is due to low specific impulse, poor propellant utilization, or a combination of both is not possible. Since the engine shutdown was caused by exhaustion of one or both of the propellants, a supposed negative error in flow rate indicates that the residual propellant weight would be higher than calculated. For an error of -1.2 percent in flow rate the figure shows that the specific impulse would be 281 seconds with a complementary 79 pounds increase in vehicle burnout weight. The figure also shows that a positive flow rate error is limited at 0.75 percent and a burnout weight of 50 pounds less than calculated. At this point, both the oxidizer and the fuel tank are completely empty.

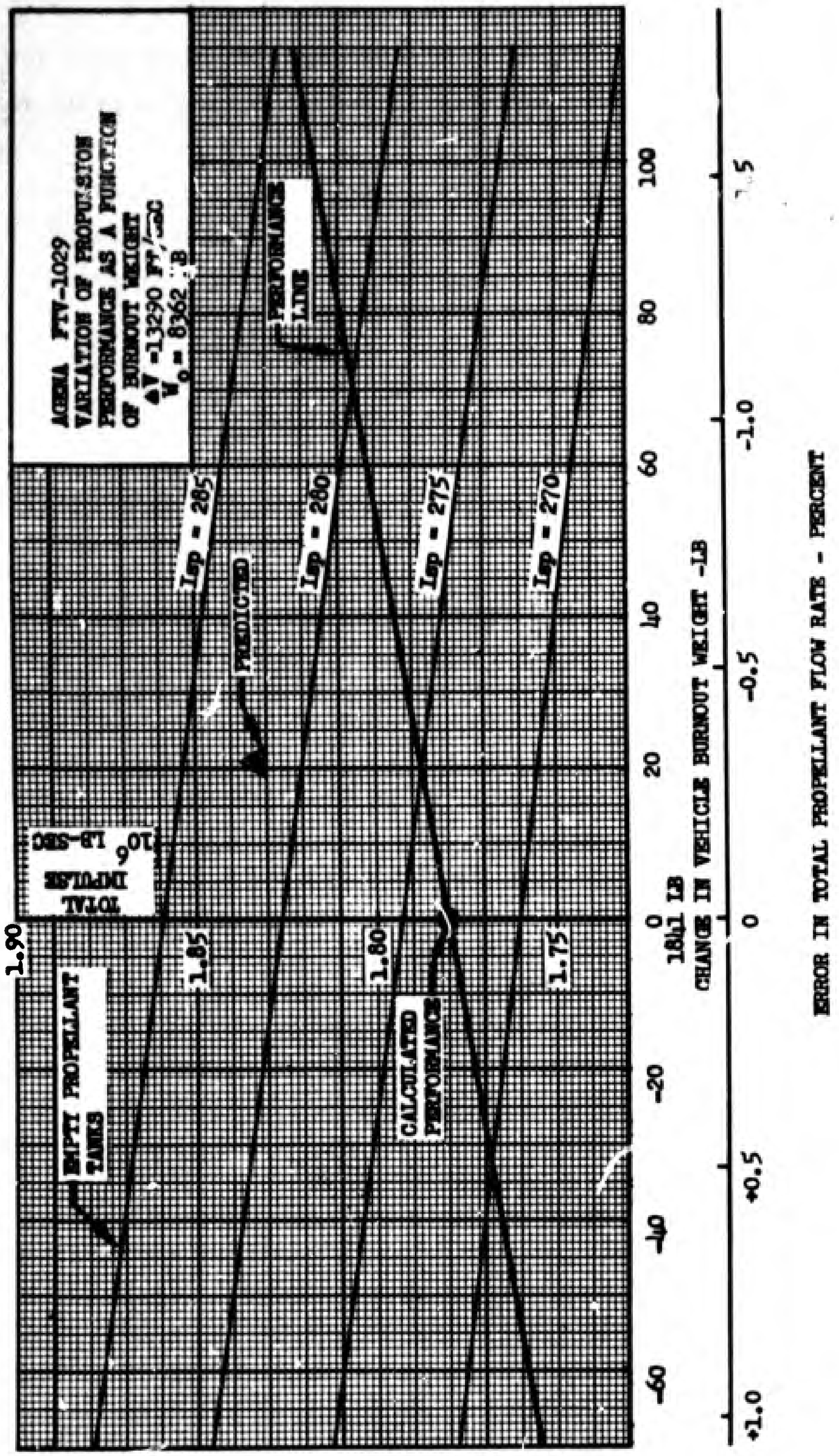

Fig. 7-2 Propulsion Performance Function Variables

A more reasonable limit of the positive flow rate error would be at 0.2 percent when the nominal residuals would exist if the oxidizer and fuel flows were in optimum ratio, such that each nominal residual would be reached at the same time.

Therefore, the actual burnout weight would be between 1829 pounds (1841-12) and 1919 pounds (1841+78). The indicated performance extremes would be 272 seconds specific impulse, with very good propellant utilization; to 281 seconds specific impulse with poor utilization. Lacking additional data, determination of the actual specific impulse-propellant utilization combination is not possible. Figure 7-3 is a summarization of engine performance parameters for all Discoverer flights to date.

Pressurization System Analysis

The propellant tank pressurization system performed as predicted and was within specification in all respects. The helium supply tank volume was changed as a result of the weight saving program. Previous flights had been equipped with two tanks of 2200-cubic-inch volume each. FTV-1029 had one 2200-cubic-inch tank, but the other tank was replaced with a 1728 cubic inch tank which was lighter in weight. The resultant decrease in volume was 10.7 percent. However, satisfactory supply was available to maintain propellant tank pressures at the required level throughout powered flight.

FTV	P_c	Flow Rate Wt	W_{ox}	W_f	I_{sp}	Burn Time Sec	I_t	ft/Sec ΔV	RPM	Residual Usable Fuel	Residual Usable Ox	Thrust lbs	Accel. Burnout g	Thrust Term.
PROPULSION PRE-FLIGHT NOMINAL Based on oxidizer runoff														
1022	501	57.21	46.29	10.92	268.0	98.3	1.50×10^6	13,436	23,380	---	---	15,350	---	
1018	491	53.8	38.6	15.2	283.0	117.5	1.80×10^6	13,990	24,050	---	---	15,260	8.8	
1020	494	54.5	39.2	15.3	283.0	118.4	1.83×10^6	14,000	24,230	---	---	15,450	8.9	
1023	500	55.8	40.09	15.78	280.6	115.5	1.81×10^6	13,460	24,440	---	---	15,660	8.33	
1029	511	56.47	40.76	15.71	282.1	115.1	1.833×10^6	13,630	24,952	14(1)	---	15,930	8.6	
PROPULSION POST-FLIGHT DATA														
1022	515.7	58.97	47.71	11.26	268.0	96.3	1.522×10^6	13,660	No Data	---	---	15,800	---	~~Type Com~~ Prop Exh
1018	505.0	55.85	40.25	15.6	281.2(1)	110.96	1.74×10^6	13,190	24,585	29	106	15,700	8.4(3)	Typ. Com ~~Typ. Com~~
1020	487.9	53.60	38.6	15.0	283.2	115.5	1.75×10^6	12,986	23,740	89	0	15,170	7.8(3)	Fuel Depl.
1023	479.0	55.60	39.9	15.7	270(2)	115.62	1.735×10^6	12,830(2)	24,113	9	10	15,010(4)	---	~~Non Deter.~~ Prop. Exh.
1029	498.0	56.46	40.73	15.73	273.0	115.49	1.78×10^6	13,320	24,670	9	10	15,610	---	Prop. Exh.

(1) P_c Monitor Suspect
(2) Digital Computed
(3) P_c and Wt
(4) Trajectory Simulation of Radar Data

Fig. 7-3 Summation of Engine Performance Parameters

SECTION 8
AUXILIARY POWER SUPPLY (SUBSYSTEM C)

Telemetry data obtained for the ascent and orbital phases, as recorded at VAFB and the telemetry ship, indicated that all components of the auxiliary power supply (including temperature measurements at the 2000 cps inverter and battery bus) operated well within specified limits. Voltage regulation was good throughout, although 400 cps and 28 cps modulations were detected on all telemetry traces. However, no deleterious effects on the performance of the equipment could be observed as a result of this modulation.

Proper activation of the hydraulic motor was noted, and firing of the separation bolts occurred as scheduled, with full battery voltage recovery indicated by the separation monitor after vehicle separation.

Telemetry records indicated typical voltage levels as shown in Fig. 8-1.

Preflight computations, based on a 56 sample statistical evaluation and using the lower 3-sigma probability evaluation of battery life, indicated a total available energy for one Type IA and one Type IIA batteries as 8,500 watt-hours, or a net usable energy of 7,750 watt-hours. Telemetry records, however, indicated that sufficient battery capacity remained beyond the recovery pass (Orbit 17) to provide power through Orbit 26 for a total power output of 11,250 watt-hours. A comparison of actual battery life with predicted battery life is shown in Fig. 8-2.

Figure 8-2 shows that an upper 2-sigma criteria applied to the batteries resulted in a total battery capacity of 11,394 watt-hours (an excess capacity of 144 watt-hours over the actual capacity). If a comparison is made

Power Source	Nominal and Tolerable Design Values (volts)	Supply Voltages Launch	+400 sec	Orbit 9	Orbit 17	Orbit 26
Battery Bus	28.0 (22/29.25)	28.0	25.3	24.3	-	21.5
(-)28V Supply	-28.3 (-27.7/-28.9)	-	-	-	-28.9	-28.7
400 cps AB ϕ	115.0 (114/116)	115.0	115.0	119.3	119.5	117.0
400 cps BC ϕ	115.0 (114/116)	116.0	116.0	-	-	116.0
2000 cps 1ϕ	115.0 (109/121)	114.8	114.2	114.0	114.0	117.0
+28V Reg*	28.0 (27.7/28.9)	27.5	27.1	27.0	27.0	27.2

*Land line data indicated 28.4 volts at launch.

Fig. 8-1 Power Requirements and Supply Voltages

		Watt-Hours
Total actual power consumed (through Orbit 26)		11,250
Predicted power consumption (Battery Types IA and IIA) (Predicated on (-) 3-sigma battery life)		7,750
Recapitulation of probable battery life (Predicated on (+) 2-sigma battery life)		
Average battery voltage (FTV-1029)	26 volts	
Average capacity (Battery Type IA)	348 A.H.	9,050
Average capacity (Battery Type IIA)	45 A.H.	1,170
Total average battery capacity		10,220
(+) 2-sigma capacity (Battery Type IA)	37.4 A.H.	972
(+) 2-sigma capacity (Battery Type IIA)	7.8 A.H.	202
		1,174
Total probable battery capacity		11,394
Excess of probable over actual battery life		144
Excess of actual over average battery life		1,030

Fig. 8-2 Comparison of Actual vs. Predicted Battery Life

between the actual and the average battery life, the actual battery life will exceed the average by 1,030 watt-hours. It is evident, therefore, that the capacity of the batteries installed in FTV-1029 fell between the average and upper 2-sigma limit (design tolerances). Figure 8-3 is a tabulation of power consumption by orbits.

	Watt-Hours		Watt-Hours
Ascent	305	Orbit 13	313
Initial Orbit	129	14	313
Orbit 1	488	15	488
2	488	16	488
3	313	17	488
4	313	18	313
5	313	19	313
6	313	20	313
7	313	21	313
8	313	22	313
9	488	23+	313
10	488	24+	739
11	488	25+	739
12	313	26+	739
		Total Energy Consumed	11,250

+ T/M and Acquisition Beacon on 100 percent duty cycle.

Fig. 8-3 Total Power Consumption by Orbits

In view of the foregoing, the lower 3-sigma method of evaluating minimum battery life is being continued at the present time as a criteria for determining battery capacity to assure sufficient power availability for carrying out flight objectives. Periodic statistical re-evaluations of battery life will continue and the results applied toward modification of present minimum battery requirements, and MIDAS and Samos Programs total battery module requirements.

SECTION 9
GUIDANCE AND CONTROL (SUBSYSTEM D)

INTEGRATOR PERFORMANCE

Time-to-Fire and Velocity-to-be-Gained

At the end of Agena engine burnout, the integrator was asking for 268 ft/sec more velocity (approximately one quarter null). An apparent discrepancy existed in velocity-to-be-gained between the transmitted command and the integrator response (Fig. 9-1).

Nineteen pairs of position coordinates of the vehicle during the coast phase (as indicated by the digitalized raw radar data from Point Mugu) have been statistically analyzed on the 1103AF computer. The results showed that the proper commands required to achieve mission objectives (perigee injection and 95.295 minute period) were a time-to-fire delay of 32.8 ± 0.7 seconds and a velocity-to-be-gained of 13,469 ± 8 ft/sec. Also, the 1-sigma noise levels in these two computations due to radar noise were 3.1 seconds and 37 ft/sec, respectively.

Actual commands computed by the Reeves Computer during the flight were 35 seconds of "D" timer delay and 13,535 ft/sec integrator velocity-to-be-gained, which showed probable errors of 2 seconds and 66 ft/sec, respectively. The major portion of these errors is believed to be because of the Reeves Computer having sampled radar data at a time when data were in the midst of a noise peak. The radar plot board showed a fairly large peak in the vicinity of the "first look" point for the computer. A much smaller portion is believed to be due to non-linearities resulting from the large deviation of the ascent trajectory from nominal. The relative importance of these two is estimated to be in the ratio of 10 to 1.

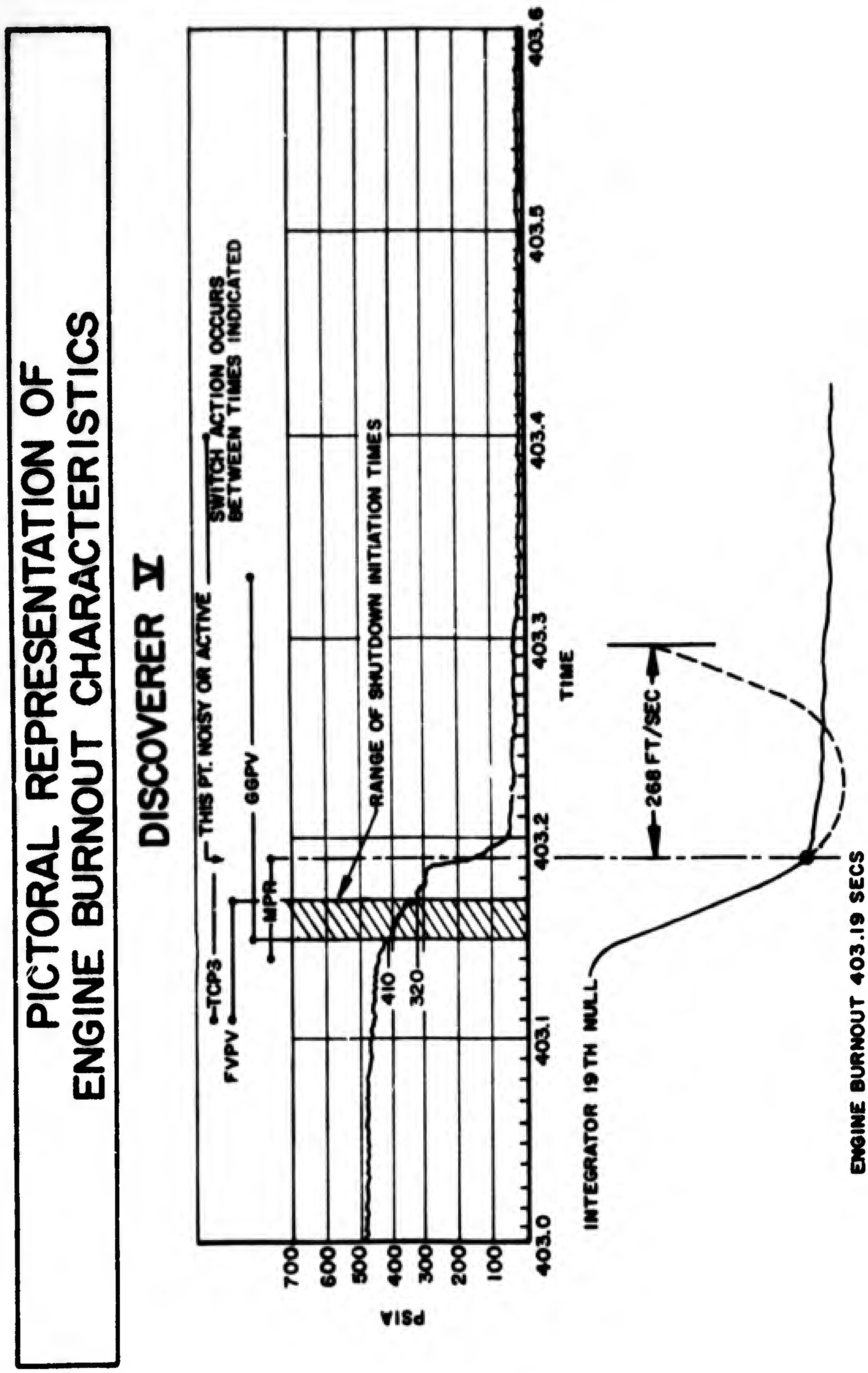
PICTORAL REPRESENTATION OF
ENGINE BURNOUT CHARACTERISTICS
DISCOVERER V
FVPV
TCPS
THIS PT. NOISY OR ACTIVE
SWITCH ACTION OCCURS
BETWEEN TIMES INDICATED
GGPV
MPR
RANGE OF SHUTDOWN INITIATION TIMES
410
320
PSIA
700
600
500
400
300
200
100
403.0
403.1
403.2
403.3
403.4
403.5
403.6
TIME
268 FT/SEC
INTEGRATOR 19TH NULL
ENGINE BURNOUT 403.19 SECS

Fig. 9-1

An error analysis of the Reeves Computer and the vehicle integrator is shown in tabulated form as Fig. 9-2. Note that a close correspondence existed between the velocity correction error and the velocity command discrepancy. The error in correction velocity of approximately 40 ft/sec was greater than that evidenced on prior flights. However, apparent corrections have been consistently smaller than command corrections which indicates the possibility of compensating for apparent system lags. Feasibility investigations are under way for applying nominal or proportional compensation of command times to correct this condition.

The flight-path angle at injection was +0.02 degree which satisfied well the requirement of perigee injection (within tolerances), even with the two-second error in time-to-fire.

Horizon Scanner

The horizon scanner installed on FTV-1029 contained a scanning head with a scan angle of ± 6 degrees and was designed for use on 89 minute period flights. This configuration provided continuous scanning of the horizon up to an altitude of 220 miles. At altitudes above 220 miles, the horizon would drop below the "look" angle of the scanner and angular displacements of the vehicle, with respect to the local horizontal in pitch and roll, would be required for the scanner to see the horizon. An analysis of the actual case of FTV-1029 showed these angles to be ± 6.2 degrees at apogee gradually decreasing to essentially zero at points ~~60 degrees from the perigee latitude.~~ Under these conditions, the scanner control system had sufficient time to make necessary corrections to the vehicle attitude during each orbit. Confirmation of corrections was obtained by Orbit 16 data from VAFB which indicated that the vehicle was cycling around a zero attitude error in pitch and roll. Since the capsule ejection sequence was initiated at an altitude well under 220 miles, adequate scanner corrections in vehicle attitude were provided. A ± 10 degrees scan angle head was installed on Agena FTV-1028 (Discoverer VI) to extend the range of the scanner; therefore, improved performance characteristics can be expected.

Integrator and Computer Error Analysis

Integrator-velocity gained (Test data)			13,310 ft/sec
Orbital period (nominal)	95.30 min.		
(actual)	94.17 "		
	1.13 "	= 100 ft/sec at injection	
Velocity gain required to attain nominal orbit period			13,410 ft/sec
Orbital period velocity gain from radar postflight analysis			13,469 ft/sec
Error in accelerometer integrator calibration			59 ft/sec
Velocity error at injection			100 ft/sec
Computer error (command correction)			66 ft/sec
Error in integrator calibration			59 ft/sec
Calculated velocity gain that should have been indicated on the integrator			225 ft/sec
Actual velocity remaining on integrator			268 ft/sec
Velocity discrepancy			* 43 ft/sec
Command velocity correction			270 ft/sec
Actual measured velocity correction			230 ft/sec
Velocity correction error			* 40 ft/sec

Error Summation-Velocity-to-be-Gained

Error in Command 6 velocity correction	66 ft/sec
Error in integrator response to Command 6	40 ft/sec
Apparent error in integrator calibration	59 ft/sec
Apparent total error	* 165 ft/sec
Velocity remaining on integrator after engine burnout	268 ft/sec
Additional velocity required for nominal orbit	-100 ft/sec
Actual total error	* 168 ft/sec

* Close correspondence between the velocity discrepancy and velocity correction error

Fig. 9-2

Control Performance and Gas Expenditure

Thrust and attitude control performance during ascent and orbital boost was within the specified limits as shown in Fig. 9-3.

The control gas expenditure was generally as predicted, except the ascent phase expenditure was substantially less than the previous average. As a result, only 80 percent of the available impulse was expended up to and including the recovery phase of the mission as determined from Orbit 17 data from Hawaii. Typical ascent phase expenditure would have added 10 percent to the total, resulting in a 90 percent expenditure of available impulse.

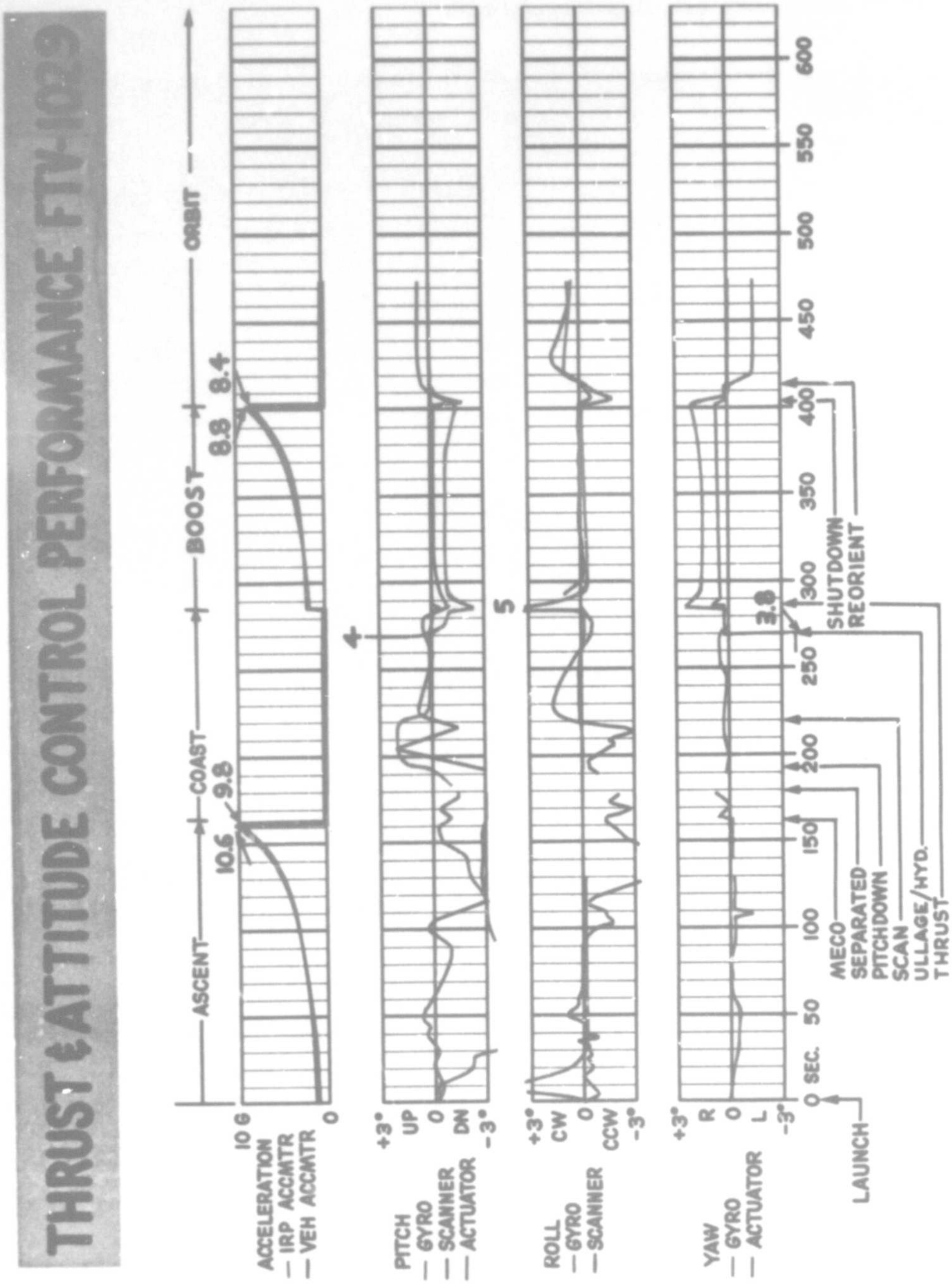
THRUST & ATTITUDE CONTROL PERFORMANCE FTV-1029
ASCENT
COAST
BOOST
ORBIT
10.6
9.8
8.8
8.4
4
5
2.8
ACCELERATION
— IRP ACCMTR
— VEH ACCMTR
10 G
0
PITCH
— GYRO
— SCANNER
— ACTUATOR
+3°
UP
0
DN
-3°
ROLL
— GYRO
— SCANNER
+3°
CW
0
CCW
-3°
YAW
— GYRO
— ACTUATOR
+3°
R
0
L
-3°
0 SEC.
50
100
150
200
250
300
350
400
450
500
550
600
LAUNCH
MECO
SEPARATED
PITCHDOWN
SCAN
ULLAGE/HYD.
THRUST
SHUTDOWN
REORIENT

Fig. 9-3

SECTION 10

GROUND-SPACE COMMUNICATIONS (SUBSYSTEM H)

TRACKING PERFORMANCE

The functions and performance of the Ground-Space Communications System (Subsystem H) were normal with the exception of some difficulty experienced during launch between the VERLORT radars and the vehicle beacon. Difficulty was also experienced with commands sent from Kodiak during the second orbit. In all subsequent periods, transmitted commands were received and executed and satisfactory examples of radar tracking were received by the tracking stations.

BEACON PERFORMANCE

Interference Problems

Functioning as a transponder, the Agena beacon receives a time-coded pulse pair from the interrogating radar. Each pulse fires a blocking oscillator having a recovery (or dead) period of nominally 4 microseconds. The blocking oscillator output of the first pulse starts an accurately timed multivibrator (which forms the coincidence point for the second pulse). Accordingly, a gate opens which allows the blocking oscillator output of the second pulse to fire the beacon transmitter and answer the radar with one transmitted pulse. Any signal arriving outside of these two-pulse times will not fire the transmitter, but should one arrive 1 microsecond ahead of the second pulse, the input circuits will be blocked. The beacon has a high sensitivity for equipment of this size and design and very weak signals within the proper frequency band. Beacon design provides for tracking at extreme distances (15,000 to 20,000 statute miles theoretically). Therefore, a radar signal of the approximate frequency of the beacon and originating nearer than 400 miles will be received. If the pulse happens to fall within the 4-microsecond period before either of the two pulses is received, the beacon will be disabled. Should this condition occur more often than 50 percent of the time, the ground tracking radar receives insufficient signal voltage to drive tracking servo systems.

During the launch of FTV-1029, several powerful radars were illuminating the vehicle beacon and disabling it more often than the VAFB VERLORT radar could tolerate (see Fig. 10-1). In past flights, this difficulty has been avoided by silencing all radar operation in the area (roughly 500 miles from the vehicle during launch and ascent periods) whenever the frequency was within 20 to 30 megacycles of the beacon receiving frequency. Records of the past flights show that the beacon receiver reacted to some interference, but none of the signals arrived to trigger the transmitter at the correctly timed 4-microsecond point. Confusion concerning the protection requirements for this flight resulted in heavy interference which was universal and continually affected the transmitter. AGC records from VAFB show that only 10 to 50 percent of the interrogations were answered, which condition reduced the lock-on signal drastically. As a result, during ascent the VAFB radar lost track for two distinct long periods of time. VAFB reported that the radar was locked-on to the beacon signal at liftoff. At T+60 seconds, heavy interference was responsible for a 50 percent countdown observation. At T+84 seconds, the countdown interference was increased to 95 percent and automatic lock-on was lost; however, tracking was continued manually.

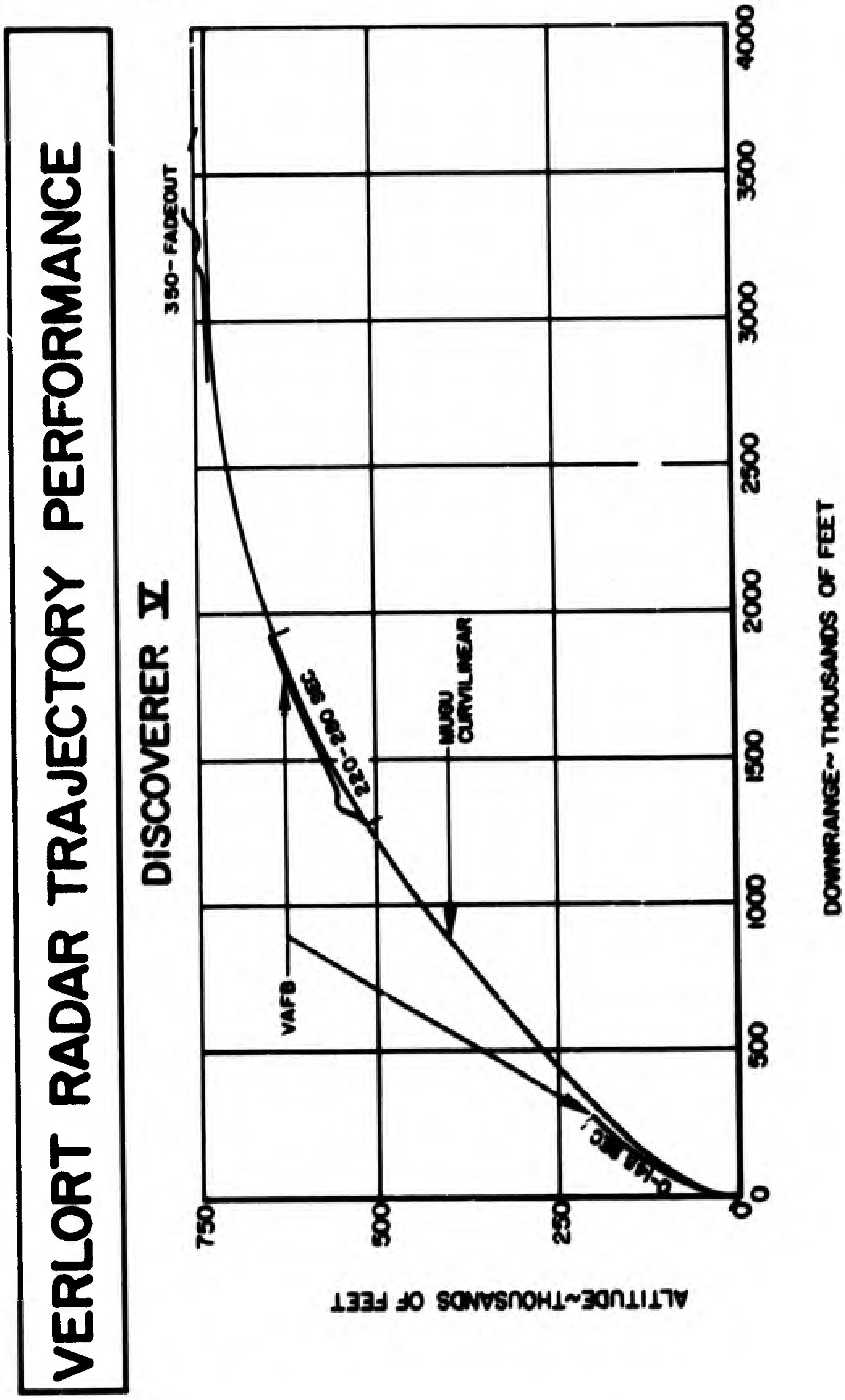
VERLORT RADAR TRAJECTORY PERFORMANCE
DISCOVERER V
350-FADEOUT
220-280 SEC
MUGU CURVILINEAR
VAFB
0-145 SEC
ALTITUDE~THOUSANDS OF FEET
750
500
250
0
DOWNRANGE~THOUSANDS OF FEET
0
500
1000
1500
2000
2500
3000
3500
4000

Fig. 10-1

At T+100 seconds, track was lost which was probably because of incoming signal loss and the return pulse not being within the range track of the gate. Accordingly, the antenna swerved upward, but tracking was resumed by slaving the radar antenna to the TLM-18. Later, the elevation error signal amplifier was found to be in an unbalanced condition; therefore, when the signal was lost, the antenna elevation went off track entirely. When Point Mugu changed PRF, the excessive interference made observation of the return pulse difficult. This condition led to difficulty in keeping the pulse within the limits of the gate. During some of the PRF changes, the Point Mugu beacon return occurred at the same range as that of VAFB. This condition caused loss of range tracking and misdirection of the antenna. VAFB went passive at T+431 seconds to eliminate interference with Point Mugu tracking.

Command Problems

The decoding function of the beacon is accomplished in much the same way as the transponder function. The first and middle pulses of the three-pulse transmitted signal to the beacon accomplish this function. The first pulse starts a multivibrator in the decoder as well as in the transmitter. The period in the decoder is set to a shorter cycle, which sets up a coincidence point for the center pulse, thus rejecting any signal not adjusted to the proper pulse-spacing to a ±0.25 microsecond tolerance. Voltage is furnished to the various command relays by the amount that the center pulse is time-modulated by audio tones, so that any absence of modulation could cause certain command relays not to close and the command would be lost. Over-modulation would cause the pulse to get into the 4-microsecond dead period of the third pulse and cause the transmitter to miss a return firing. Accordingly, the amount of modulation is extremely critical. If an interfering radar signal is received into the beacon receiver within 4-microseconds of the center pulse, the command signal for that pulse group is lost, since the blocking oscillator will not accept a pulse again until the dead period passes. During the second pass of the vehicle over Kodiak, six Number 2 commands were transmitted to step the timer. Each time a command was received by the beacon, the transmitter refused to answer the interrogating radar during that period, because the command tone (middle) was apparently too close to the third pulse and was within the 4-microsecond period as it was modulated. No serious damage was caused, but satisfactory tracking records were difficult with the beacon transmitter going off the air when commands were sent. Had this been one of the radars used during ascent, conceivably the sending of Command 5 could have kept the transmitter off, causing tracking to be lost. One of two difficulties with the ground radar could have caused this effect: (1) the center pulse may have been modulated too widely (possibly out of the 0.5-microsecond tolerance) or (2) the pulse spacing may have been outside of tolerance. When all tolerances were added together, a safety margin of only 0.75 microsecond remained, which was too close. Modulation limits of the center pulse will be lowered to eliminate this difficulty, and center pulse spacing will be checked more carefully.

Outside interference can cause command difficulties, as previously explained. Command 5 was seen to drop out for three seconds after having been sent by Point Mugu. Although this dropout was probably caused by the heavy interference experienced by the beacon during the launch phase, no effect was evidenced on the D-timer brake hold time, because the orbital timer, as a backup, also holds on the brake during the first 20 seconds of Command 5 time.

BLANK PAGE

SECTION 11
INSTRUMENTATION

The instrumentation and telemetry data link on FTV-1029 performed according to design with the exception of five lost measurements during the launch phase and all of Channel 12 (24 measurements) after Orbit 2. Cause of the Channel 12 lost measurements was apparently due to failure of the differential amplifier. Data recovery and the amount of usable data are summarized in

Type Measurement	No. Made	No. Lost	Data Pt. Recovery (%)	No. Yielding Inadequate Data	Adequate Data (%)
Primary	34	0	100.0	0	100
Secondary	125	4	97.0	3	96
Tell-tale	15	1	93.3	0	93
Total	174	5	97.1	3	95

These figures do not include the loss of Channel 12 measurements (24 quantities) after the second orbit.

Fig. 11-1 Summary of Instrumentation Performance

A problem area existed in the temperature measurements as evidenced by recorded data which indicated shifts from the expected nominal values at liftoff. Further analysis will be conducted to locate the cause of these deviations.

Figures 11-2a and 11-2b show the received signal strength at VAFB.

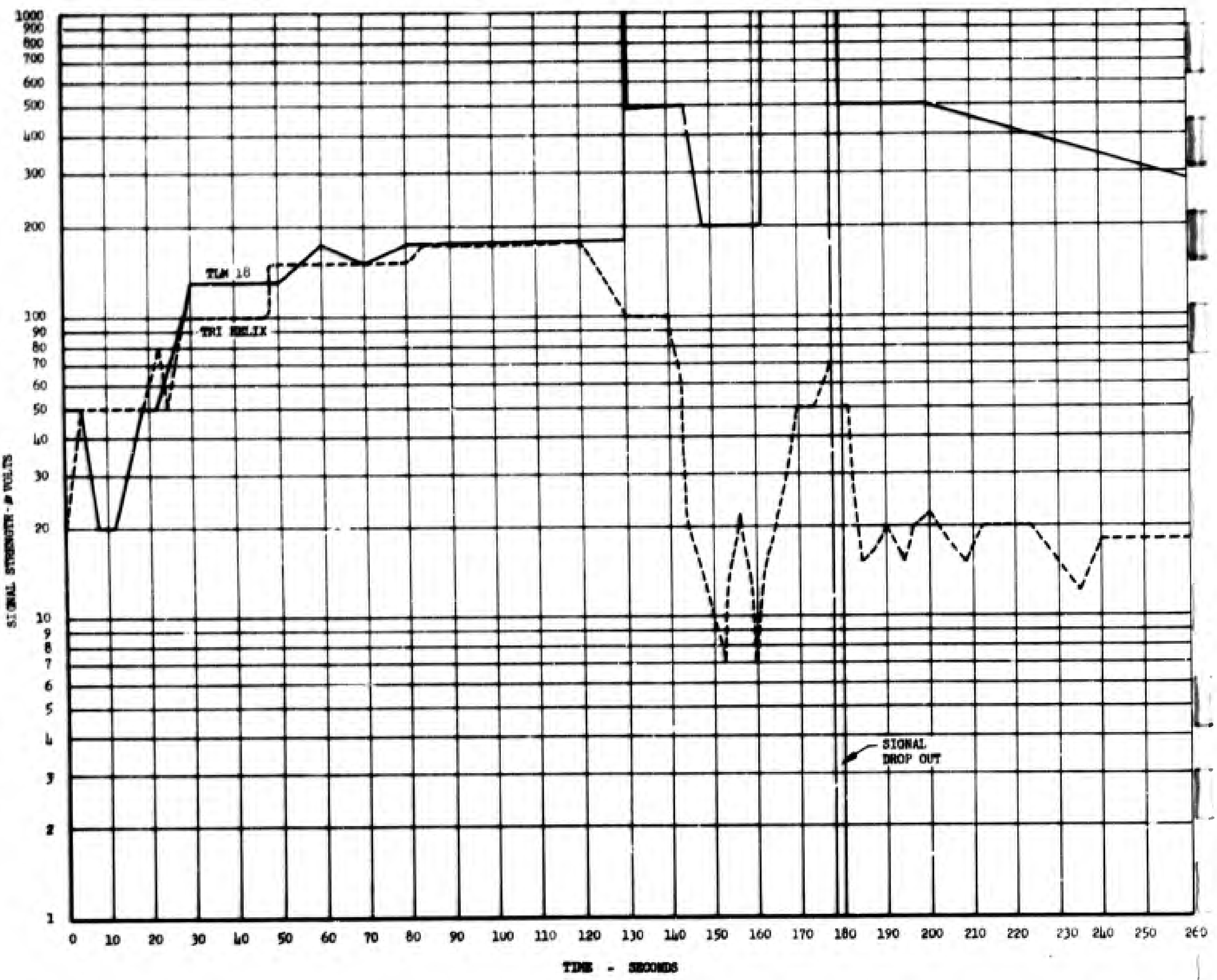

Fig. 11-2a Telemetry Signal Strength vs Time From Launch

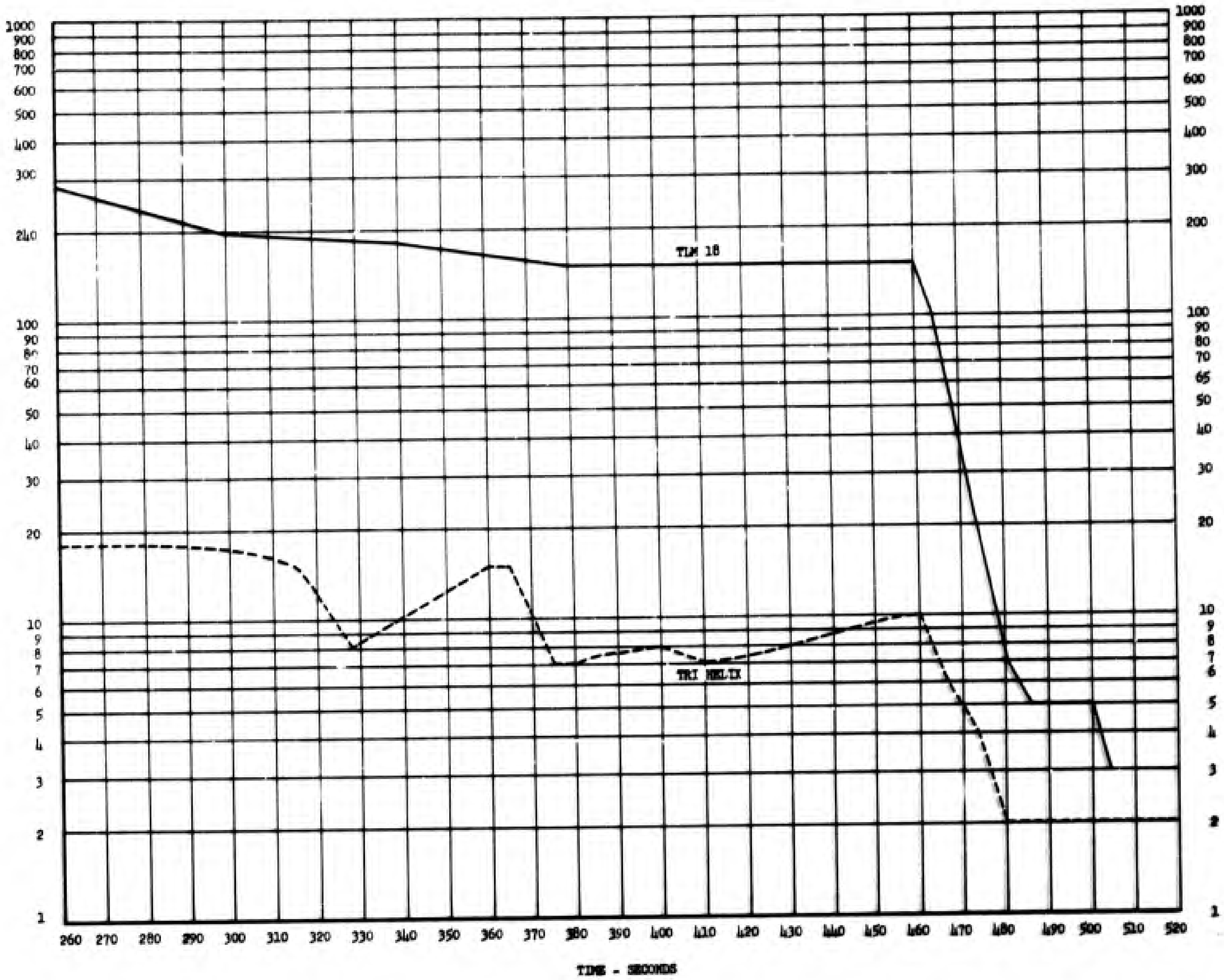

Fig. 11-2b Telemetry Signal Strength vs Time From Launch

Analysis was made on the basis of lost measurements and questionable data reported by Data Services, Data Analysis, Subsystem A, and Subsystem B. Those measurements which have been reported as questionable are:

a. A 74, Forward Compartment Pressure
b. B 3, Gas Generator Chamber Pressure
c. B 19, Oxidizer Manifold Pressure
d. H 71, Telemeter Transmitter Temperature
e. SD 103, Helium Sphere Compartment Temperature
f. All Channel 12 measurements after Orbit 2
g. SD 39, 40 and 41, skin temperatures.

An analysis of each follows:

Problem: The Forward Compartment Pressure (A74) failed to read ambient pressure with increase in altitude.

Condition: Pressure at launch read close to sea level, then gradually approached zero, as indicated by the data for Orbit 1.

Conclusion: The extremely slow response to ambient pressure conditions suggests that the protective plastic dust-cap may have been left on the pressure-sensing part of the transducer.

Problem: The Gas Generator Chamber Pressure (B3) failed at approximately 320 seconds.

Condition: Data obtained from this position indicated normal operation until 320 seconds. At that time, the commutated traces go below bandwidth limits.

Conclusion: Valid data were recorded from 0 to 320 seconds. Measurement loss at this time was because of the possible broken lead at the pressure transducer.

Problem: The Oxidizer Manifold Pressure Switch (B19) failed to indicate.

Condition: The commutated trace exhibited no indication of floating and remained at zero.

Conclusion: Cause of failure was because of an open circuit from the voltage source to monitor circuit. Tell-tale indication was lost.

Problem: Telemeter Transmitter Temperature (H71) read out of band.

Condition: Commutated trace indicated an open bridge.

Conclusion: Measurement was lost.

Problem: Helium Sphere Compartment Temperature (SD103) read 300^{o}F at liftoff.

Condition: The time versus temperature data indicated normal operation except for quantitative values.

Conclusion: Temperature shift was applied and data were utilized at reduced accuracy.

Skin temperature thermocouple data were not valid. The exact cause is unknown.

BLANK PAGE

SECTION 12
RECOVERY RESEARCH CAPSULE (SUBSYSTEM L)

Separation of the Recovery Research Capsule from the Agena vehicle occurred as programmed by the Subsystem L Timer at 2140:09 GCT on Orbit 17. This was verified by telemetry data. Spin and retro-rocket firing was verified by a temperature rise indication from the vehicle forward thermocouples. Subsequent events in the normal re-entry and lower atmosphere recovery sequence can not be substantiated (see Fig. 12-1). The visual and electronic aids, such as parachute and chaff, deployment acquisition beacon, and signal light circuits, were apparently not activated. Since records of events beyond initial separation are not available, the exact cause of the second-stage failure cannot be determined; however, it is believed to have been due to lower-than-predicted temperature effects on the Mercury-type batteries which power the interstage separation circuits.

Corrective action, consisting of removal of the outer paint covering from the ablative shell, will be accomplished prior to the next scheduled flight. It is believed that this will permit absorption of enough solar energy to raise the internal capsule temperature to safe battery-operating limits.

Recovery was not accomplished, and after continued surface search over the predicted impact area for three days, the capsule was presumed lost. Accordingly, the search was abandoned.

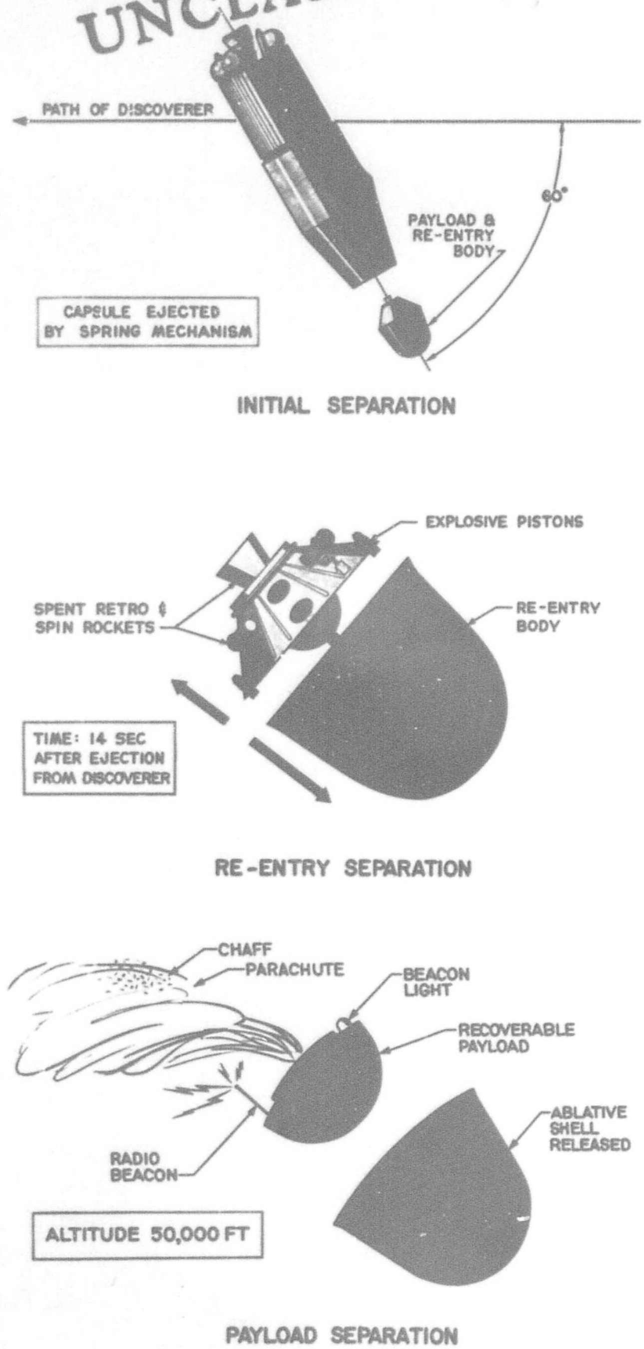

Fig. 12-1 Re-entry and Recovery Sequence

REFERENCES

1. Performance Analysis Report, Flight of FTV-1023, LMSD-445052, 25 July 1959
2. Detailed Test Objectives, Flight 6, LMSD-6155-6, 30 May 1959
3. Preliminary System Test Report (5 day) Discoverer V, LMSD-6149-6, 23 August 1959
4. General Environment Specification for Discoverer, MIDAS, and Sentry Programs, LMSD-6117A, Revision 24 June 1959
5. Subsystem B Engineering Analysis Report, UDMH Fueled Engine, LMSD-422245, 30 November 1958
6. Propulsion Subsystem Specification (UDMH Configuration) for Discoverer Program, LMSD-6161, 30 March 1959
7. PMR Metric Optical Data, LMSD-445776, 16 August 1959
8. Performance Analysis Report, Flight FTV-1020, LMSD-445051, 3 July 1959